SGG SGS sc | nat
Swiss Journal of Geosciences

ORIGINAL PAPER Open Access

Metamorphic gabbro and basalt in ophiolitic and continental nappes of the Zermatt region (Western Alps)

Kurt Bucher* and Ingrid Stober

Abstract

The composition of meta-gabbro and meta-basalt occurring abundant and widespread in all nappes of the nappe stack exposed in the Zermatt region of the Western Alp shows distinct patterns related to the geodynamic origin of metamorphic basic rocks. Eclogitic meta-basalts of the ophiolitic Zermatt-Saas Unit (ZSU) show enriched MORB signatures. The meta-basalts (eclogites) of the continental fragment of the Theodul Glacier Unit (TGU) derive from pre-Alpine metamorphic continental intraplate basalts. Meta-basalts (eclogites) from the continental basement of the Siviez-Mischabel nappe (SMN) derive from MORB thus a genetic relation to the TGU eclogites can be excluded. All basic igneous rocks experienced post-magmatic alteration by fluid-rock interaction ranging from processes at the seafloor, in the shallow crust, during subduction zone hydration, in the exhumation channel and late Alpine regional metamorphisms. The consequences of these alteration processes can be identified at various levels in the rock composition data. It was found that the REE data are little affected by fluid-rock alteration. Some trace elements, notably Cs, Rb, and Ba are typically massively altered relative to igneous compositions in all three groups of meta-basalts. Generally, meta-basalts from the TGU and the SMN preserved the features of the original composition whilst the ZSU meta-volcanic rocks experienced massive alteration. For the ZSU meta-volcanic rocks it is evident that Zr was gained and Y lost during high-pressure fluid-rock interaction indicating a mobile behavior of the two elements during HP-metamorphism in contrast to their behavior in hydrothermal near-surface fluid-rock interaction.

Keywords: Meta-basalt, Meta-gabbro, Trace elements, REE patterns, Ophiolite

1 Introduction

The composition of both intrusive and extrusive basic igneous rocks shows characteristic properties of the geodynamic environment of the melt production (e.g. Cruciani et al., 2015; Fourny et al., 2019; Hollocher et al., 2016; Pedersen & Hertogen, 1990; Plank & Langmuir, 1988; Sun & McDonough, 1989; Yaliniz, 2008). The composition patterns of major, trace and rare earth elements have been widely used for characterizing the geodynamic setting particularly of both continental and oceanic basaltic lava and their metamorphic products (e.g. Coish et al., 2015; Pedersen & Hertogen, 1990; Will et al., 2015). The composition patterns of basalts reflect the mantle source, the tectonic setting of the extrusion environment, mixing with other melts and other geological aspects (Gale & Roberts, 1974; Grenne & Roberts, 1980). Composition patterns of gabbros have also been successfully used for deciphering the geological environment of the magma chambers where the gabbro formed (Fourny et al., 2019; Franciosi et al., 2019; Hollocher et al., 2012). IODP ocean drilling efforts produced composition data from gabbros together with data from dykes and lavas in a MORB environment on the fast-spreading East Pacific Rise (Neo et al., 2009; Teagle et al., 2009).

Editorial handling: Othmar Müntener.

*Correspondence: bucher@uni-freiburg.de
Institute of Earth and Environmental Sciences, University of Freiburg, Albertstr. 23b, 79104 Freiburg, Germany

Once extruded pristine basalts are susceptible to chemical and mechanical alteration by a large number of processes depending on the further geological development of the rocks. Particularly the composition of basaltic lava can be modified repeatedly (Hernández-Uribe et al., 2020; Hopper & Smith, 1996; Loeschke, 1976; van der Stratten et al., 2012). Gabbro is perhaps less susceptible to post-formation alteration, but most gabbros also show various alteration structures (Hopper & Smith, 1996). Oceanic basalt reacts with seawater producing a large variety of alteration products. One prominent basalt-seawater interaction process results in the loss of Ca and an increase in alkalis, a process called spillitization (Hernández-Uribe et al., 2020; Winchester & Floyd, 1976). Spillites are common altered basalts from oceanic environments and help to identify ophiolitic environments in the absence of pillow structures. If basic igneous rocks get involved in orogenic processes they convert to meta-basic rocks including greenschist, amphibolite and eclogite. Retrogression during exhumation of eclogite and overprinting by late collision phase metamorphism may further modify the original composition of former basalt and gabbro. Thus it is surprising that composition patterns of such highly transformed mafic igneous rocks still prove significant and useful for indicating the original geological environment of formation (Winchester & Floyd, 1976).

In the Zermatt region of the Western Alps (Fig. 1), former basaltic and gabbroic igneous rocks are an essential component in continental and oceanic thrusted units from the European plate through the former Tethys to the Apulian continental plate. The meta-basic rocks range in age from Precambrian to Mesozoic. The basic igneous rocks have been modified by processes to a variable degree depending on the tectonic position of the rocks in the folded nappe stack. The processes that acted

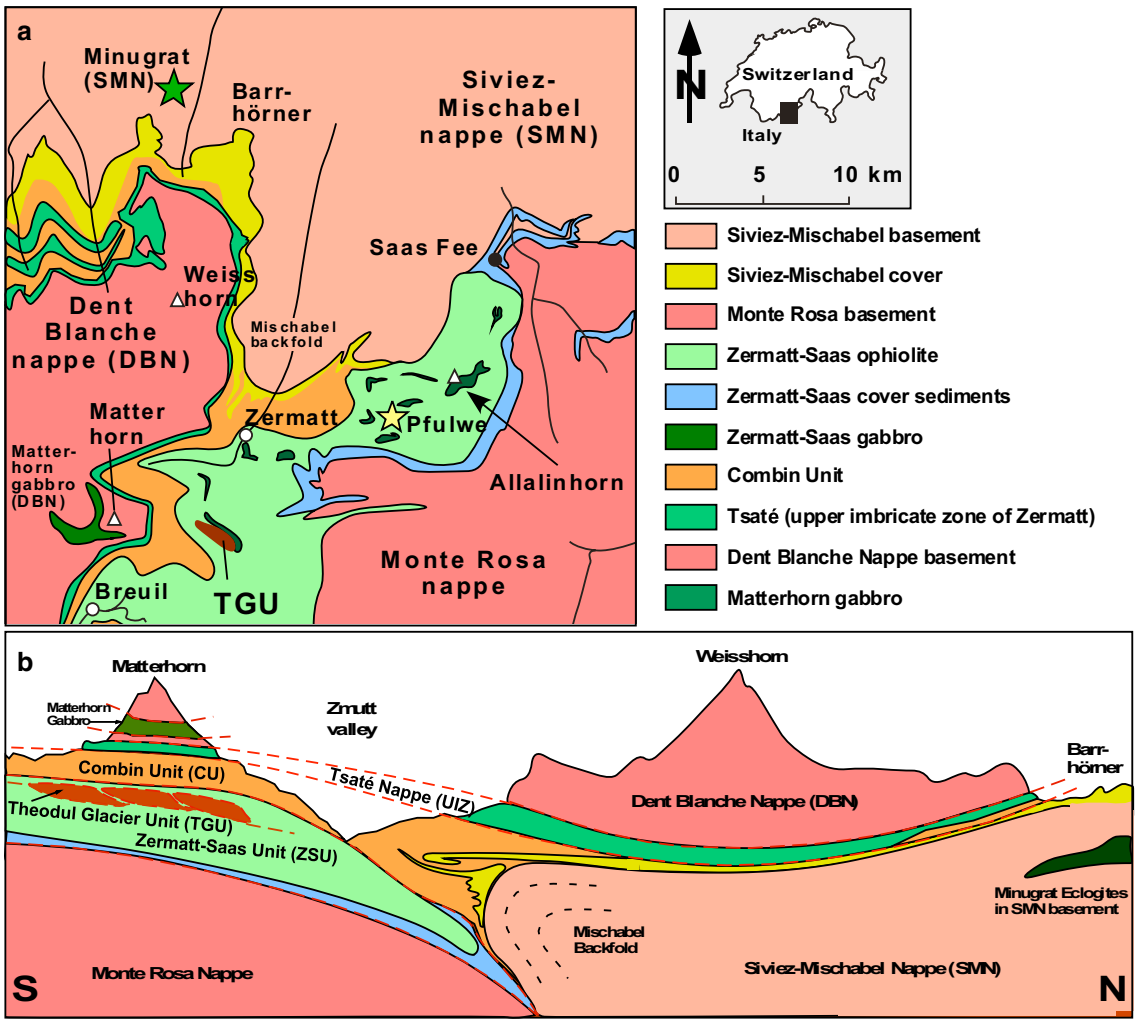

Fig. 1 **a** Simplified geologic map and **b** cross section of the Zermatt area (after Bearth, 1953, 1967, 1978; Bucher et al., 2003; Marthaler et al., 2008)

on the igneous rocks include seafloor alteration, interaction with subduction and exhumation zone fluids, low-grade fluid-rock interaction and polyphase and polycyclic metamorphism. Thus the exposed meta-basic rocks consist of greenstones, greenschists, amphibolites, eclogites and meta-gabbros including greenschist- and eclogite-facies meta-gabbros. In this paper we use major, trace and rare earth composition data from these diverse basic metamorphic rocks in an effort to identify the original geodynamic setting of basalts and gabbros and the effect the various alteration processes on the original composition of the basic igneous rocks.

2 Mafic rocks of the Zermatt region

2.1 Geological setting

The wider Zermatt region of the Western Alps exposes a unique N-S cross-section of stacked and folded nappe sheets of continental and oceanic origin (Fig. 1).

The central element is the Zermatt-Saas Unit (ZSU) representing a fully developed Mesozoic ophiolite that has been subjected to high-pressure and locally ultra-high-pressure metamorphism (Angiboust et al., 2009; Bearth, 1967; Bucher & Grapes, 2009; Bucher et al., 2005; Groppo et al., 2009; Rebay et al., 2012) during Cretaceous to Eocene subduction under the overriding Apulian plate (Bowtell et al., 1994; Lapen et al., 2003; Rubatto & Hermann, 2003; Rubatto et al., 1998). Specifically, eclogite formation in the ZSU began 44 Ma ago in the Lutetian (middle Eocene) (44.86 ± 0.49 Ma and 43.6 ± 1.8 Ma Rb–Sr ages of Ph inclusions in Grt from de Meyer et al. (2014); all abbreviations of mineral names from Whitney & Evans, 2010) and continued to the Lutetian-Bartonian boundary at 40.6 ± 2.6 Ma (Amato et al., 1999).

The oceanic rock assemblage of the ZSU consists of: (i) serpentinites representing the hydrated mantle portion of the lithosphere (Li et al., 2004a) and associated meta-rodingites (Li et al., 2004b, 2008), (ii) eclogites representing basaltic meta-volcanics, with locally well preserved primary volcanic structures such as pillows (Bearth, 1967; Bucher et al., 2005), (iii) various types of eclogite-facies meta-gabbro including ferro-gabbro (Ganguin, 1988) and the Allalin meta-gabbro (Bucher & Grapes, 2009) (Fig. 1), and (iv) subordinate amounts of oceanic sediments locally with characteristic Mn-rich quartzites, probably metacherts (Bearth & Schwander, 1981). The rock assemblage represents a typical meta-ophiolite. The ophiolites of the Tethys occurring in the Western Alps and the Apennines have been extensively studied and interpreted as generated along a slow-spreading mid-ocean ridge (Charlot-Prat, 2005; Desmurs et al., 2002; Furnes et al., 2020; Lagabrielle & Cannat, 1990; Lagabrielle & Lemoine, 1997; Manatschal et al., 2011; Li et al., 2015). The Alpine oceanic environment developed by rifting the thinned Permian–Triassic continental crust forming a ocean-continent transition zone with serpentinized subcontinental mantle and later gabbro/basalt production along the rift according to the thermo-mechanical numerical model of Marotta et al. (2018). Roda et al. (2018) proposed that the transition from Permian lithospheric thinning to continental breakup and basic magmatism was followed by an "oceanization" of the lithosphere. The Alpine Tethys in the Zermatt region started to form in the early to middle Jurassic (Stampfli, 2000; Stampfli & Marchant, 1997).

The oceanic lithosphere was consumed along an active convergent margin in the south and subducted under the continental lithosphere of the Apulian Plate beginning in Late Cretaceous but mostly in the Early Tertiary (Rubatto et al., 1998). Portions of the subducted oceanic material were returned to shallower depth along the plate contact (subduction channel) and were subsequently re-deformed and overprinted during continental collision in the Mid-Late Tertiary (Barnicoat & Fry, 1986; Barnicoat et al., 1995; Bearth, 1967). The ZSU ophiolites reached greenschist facies overprint in the Bartonian at 38 ± 2 Ma (Amato et al., 1999).

The ZSU ophiolite were incorporated in the alpine nappe stack during the late collision phases and form a large N-closing recumbent fold (Fig. 1). European continental basement and its cover units (Monte Rosa and Mischabel nappes) lie structurally below the ophiolites (Fig. 1), the Apulian continental basement (Dent Blanche nappe system) represents the structurally highest unit.

The Dent Blanche nappe system is a complex structure overriding all other nappes in the Zermatt region. The nappe consists of three major units (Argand, 1908; Bucher et al., 2003): a) banded granitoid gneisses and massive granites (Arolla series), b) pre-alpine high-grade metamorphic rocks including garnet-cordierite-sillimanite gneiss, tremolite-diopside marble and garnet amphibolite (Valpelline series) and c) large masses of meta-gabbro (Dal Piaz et al., 1977) that are included in this study. The Dent Blanche nappe system shows complex internal Alpine deformation (Bucher et al., 2003, 2004) and can be subdivided into various sub-nappes (Dal Piaz et al., 2001, 2015; Manzotti et al., 2014, 2017).

Three thin nappes between the Dent Blanche nappe (DBN) and the Zermatt Saas ophiolite unit (ZSU) are referred to as Tsaté, Cimes Blanche and Frilihorn nappe respectively (Escher et al., 1993; Pleuger et al., 2007; Steck et al., 1999). These three nappes are also collectively known under the name Combin Unit (CU). The upper part of the CU (Tsaté nappe) consists predominantly of Mesozoic metasediments, metamorphic mafic and ultramafic rocks, the lower part of the CU contains calcareous micaschists and greenschists, but also Permo-Triassic marble and quarzite (Bearth & Schwander, 1981). The

CU in the Zermatt region preserves rare blueschist facies assemblages but no eclogites (Bucher et al., 2004). The CU basal thrust (Fig. 1) is, therefore, a major discontinuity in metamorphic grade and juxtaposes two units with contrasting subduction-exhumation histories during late collision and nappe stacking.

The Theodul Glacier Unit (TGU) (Bucher et al., 2020; Weber & Bucher, 2015) is a 2×0.2 km outcrop of eclogite facies continental basement rocks within the Zermatt-Saas meta-ophiolites (Fig. 1). The Theodul Glacier Unit is named after the very rapidly retreating Upper Theodul Glacier south of Zermatt close to the Swiss-Italian border. The slab of the conspicuously rusty-weathering rocks of Theodul Glacier Unit is unique to the Zermatt region. The TGU consists predominantly of garnet-phengite schist and gneiss with associated eclogite occurring as lenses and bands within schist and gneiss. The complex internal chemical structure of garnet porphyroblasts in the Grt-Ph schist suggests a polycyclic metamorphic history of the TGU (Bucher et al., 2019). Geochronological data from the eclogites confirm the polycyclic nature of the TGU. Lu–Hf ages of 55 Ma have been derived from eclogite garnet (Weber et al., 2015), a Permian 295 Ma age has been reported for the growth of metamorphic zircon in TGU eclogite (Bucher et al., 2020). The TGU eclogites are included in this study.

The Siviez-Mischabel nappe (SMN) consists of an extensive basement core of predominantly Prealpine granite and gneiss, but also includes metamorphic mafic rocks inter alia amphibolite, eclogite and greenschist (Eisele et al., 1997; Marthaler et al., 2008; Rahn, 1991). The basement is covered by the Barrhorn series, an autochthonous cover of sediments ranging from Permian to Eocene in age (Bearth, 1978; Ellenberger, 1953). In the Zermatt area the SMN forms a large antiformal backfold closing to south (Fig. 1). The cover sediments partly detached from the basement and form imbricates that can be found considerably further south from the backfold (Bearth, 1953). It remains a possibility that also flakes from the basement including metamorphic basic rocks have been transported towards south and above the Zermatt-Saas Unit forming the TGU slab in the ZSU. For this reason some eclogite samples from the SMN have been included in this study.

In the Monte Rosa region (Fig. 1) a series of thin continental units (Furgg Zone, Portjengrat) and the Monte Rosa cover below the ZSU ophiolites contain amphibolites and other meta-basaltic rocks. These meta-basalts have not been included in this study since their setting, geology and rock composition has been documented and discussed by Kramer et al. (2003).

2.2 The samples: field occurrence, structure and petrography

2.2.1 Meta-gabbro of the Zermatt-Saas Unit (ZSU)

Meta-gabbro occurs widespread as lenses, bands and large outcrops within the metamorphic ophiolite of the ZSU. The largest meta-gabbro mass is the Allalin meta-gabbro presented separately in paragraph 2.2.2 below. Meta-gabbros of the ZSU range from Mg-rich containing no or very little garnet to Grt-rich ferro-meta-gabbro (Ganguin, 1988; Pfeifer et al., 1989). The ZSU meta-gabbros are often whitish strongly deformed rocks with prominent clinozoisite and they cannot easily be recognized as derived originally from gabbro at a given outcrop. However, the gabbro origin is evident in the field because the white Czo-schists often grade laterally into schists with clear relics of large altered augite. The meta-gabbro band below the TGU basal thrust at Trockener Steg is a typical example of very strongly altered ZSU gabbro (Fig. 2a) showing the flaser structure typical of most ZSU meta-gabbros. The dark lenses represent Amp + Chl pseudomorphs after primary augite with green cores of Omp-rich pseudomorphs (Fig. 2b). Grt is sporadically present in the whitish Clz-rich portions of the rocks. Green Cr-bearing white mica (fuchsite) occurs widespread in the meta-gabbros.

Several meta-gabbro bodies occur in the Flue-Pfulwe area east of Zermatt (Fig. 1). Samples from Spitzi Flue meta-gabbro, Fluealp meta-gabbro, and Fluehorn meta-gabbro are included in this study (Table 1). These meta-gabbros show typically a banded gneissic structure. Primary Cpx is completely replaced by a fine-grained green mass consisting of Omp + Amp + Ep (Clz). Pg, Ab and Clz form pseudomorphs after primary Pl. Grt probably formed from primary Ol and Pl and thus occurs predominantly in light colored portions of the flaser meta-gabbro. The euhedral Grt often shows replacement rims consisting of green–blue barroisitic amphibole + Clz + Chl + Pg + Mt (Fig. 3). Typically three Ti-minerals, Rt, Ilm and Tit, are present.

2.2.2 Allalin meta-gabbro of the Zermatt-Saas Unit (ZSU)

The Allalin meta-gabbro forms a prominent outcrop of 2×1 km size at the mountain Allalinhorn (4027 m) within the metamorphic ophiolite of the ZSU (Bucher & Grapes, 2009). The meta-gabbro is very heterogeneous regarding structure, grain size and mineral assemblages. The meta-gabbro has been subducted and metamorphosed under eclogite facies conditions at 44 Ma (Rubatto et al., 1998). The maximum P and T attained along the subduction—exhumation path are 2.5 GPa and 600 °C (Bucher & Grapes, 2009). During alpine subduction the meta-gabbro has been massively hydrated and the primary minerals pseudomorphed by

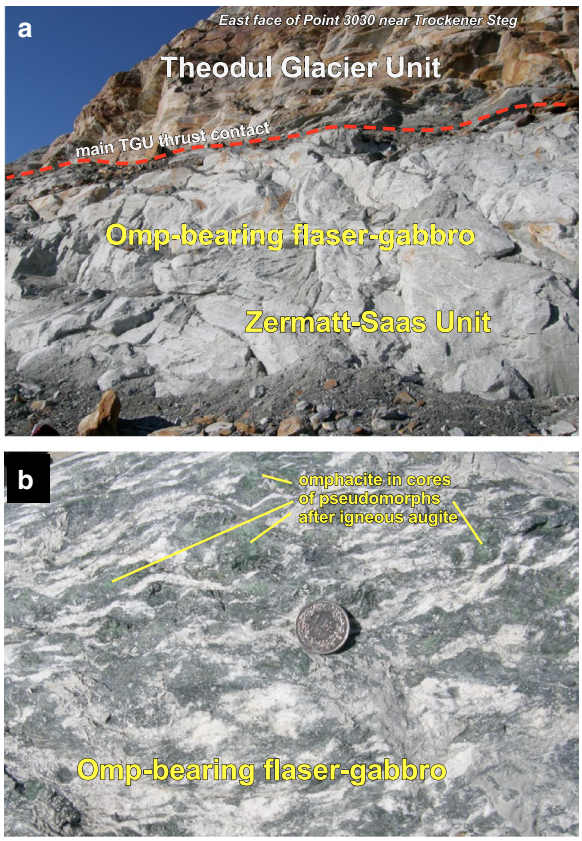

Fig. 2 Field occurrence of metamorphic gabbroic rocks. **a** East wall of point 3030 near Trockener Steg south of Zermatt. White rock = flaser-gabbro of the Zermatt-Saas unit (ZSU) separated by the basal thrust from the rusty brown Grt-Ph schists and eclogites of the Theodul Glacier unit (TGU) on top (see Fig. 1 for location of TGU). P3030 is the sampling locality of most TGU eclogites presented in this paper; **b** Close-up of the ZSU flaser-gabbro outcrop **a** with dark-green Cam + Chl patches of the post-eclogite stage representing deformed pseudomorphs after igneous augite. The augite pseudomorphs display green cores of omphacite of the eclogite facies HP stage. Sampling locality of KB1368 and KB1368

high-P assemblages. Omphacite pseudomorphs substitute augite, fine-grained aggregates of Jd + Zo + Ky + Qz pseudomorphs plagioclase (Pp = plagioclase pseudomorphs) and Tlc + Cld pseudomorphs olivine. However, primary igneous plagioclase, augite and olivine are locally preserved. A middle Jurassic (Callovian) crystallization age of 164 ± 2.7 Ma has been reported for the gabbro (Rubatto et al., 1998).

For this study six samples from the Allalin meta-gabbro have been included (Table 1). The samples have been collected in the block field (point 2940) under the 600 m high south-wall of Allalinhorn and at the E-Hohlaubgrat. Composition data for all rocks and all minerals can be found in Bucher & Grapes, 2009. Additional new rock composition data including trace elements and REE are given on Additional file 1: Tables S1–S4. The samples range from weakly transformed primary gabbro (sample numbers 875 and 876) to strongly eclogitized meta-gabbro (877 and 879) with Omp + Tlc + Cld + Pp and very intensely modified and hydrated meta-gabbro (880 and 881) rich in blue amphibole, chlorite and paragonite.

2.2.3 Meta-basalt of the Zermatt-Saas Unit (ZSU)

Mafic meta-volcanic rocks occur as greenschists, eclogites and retro-eclogites in the ZSU. Locally primary pillow structures are preserved revealing an oceanic extrusion environment. Particularly well preserved are meta-basaltic eclogites in the Fluealp area including Pfulwe pass (Fig. 1). The ZSU eclogites received much research attention and have been studied in detail after the pioneering work by Bearth (1959). Detailed petrological studies (Angiboust et al., 2009; Barnicoat & Fry, 1986; Bearth, 1963, 1967; Bucher et al., 2005; Ernst & Dal Piaz, 1978; Oberhänsli, 1982) showed that the basalts have been exposed to $P \sim 2$—2.5 GPa and $T \sim 550$—600 °C during Eocene subduction. Geochemical rock composition data (Bearth & Stern, 1971, 1979; Pfeifer et al., 1989) suggested a tholeitic MOR origin of the meta-basaltic rocks. According to the cited studies, the basalts extruded in the Jurassic possibly along a slow-spreading oceanic ridge. The basalts underwent extensive spillitization and other forms of seafloor alteration, later polyphase Alpine metamorphism associated with extensive hydrothermal alteration (Widmer & Thompson, 2001; Widmer et al., 2000). Five samples of eclogite from the Pfulwe area (Fig. 1) with very minor extent of modification during late greenschist facies metamorphism have been included in this study (Table 1). All samples contain the eclogite assemblage Grt + Omp + Czo(Zo) + Gln + Rt and an irregular amount of late Pg + Chl + Mrg + Cam. The eclogites occasionally also contain the critical UHP pair Cld + Tlc (Bucher et al., 2005) that may have formed at $P > 2.5$ GPa.

2.2.4 Meta-basalt of the Theodul Glacier Unit (TGU)

The TGU is a slab of continental rocks and includes Grt-Ph schists, and granitoid gneiss in addition to eclogite (Weber & Bucher, 2015). Mafic metavolcanic rocks occur as eclogite and retro-eclogite in lenses and bands intimately associated with Grt-Ph schists. No primary volcanic structures are preserved. The internal structure of the garnets of the Grt-Ph schists suggests a polycyclic history for the TGU (Bucher et al., 2019). The available age data from the eclogites and the derived P–T path for the TGU bears evidence for a Permian granulite facies metamorphism at 295 Ma (Bucher et al., 2020) and an Alpine subduction related eclogite facies overprint at 57 Ma (Weber et al., 2015) with subsequent retrogression.

Table 1 Sample list with coordinates of sample location

Protolith	Rock type	KB #	Locality	Geology	Unit	Northing/Easting
Meta-gabbro	HP-Meta-gabbro	1368	Trockener Steg P3030	Zermatt Ophiolite	ZSU	45°57′54.93" N 7°43′05.33" E
	HP-Meta-gabbro	1369	Trockener Steg P3030	Zermatt Ophiolite	ZSU	45°57′56.35" N 7°43′06.25" E
	HP-Meta-gabbro	1370	Fluealp	Zermatt Ophiolite	ZSU	46°00′49.42" N 7°49′00.29" E
	HP-Meta-gabbro	1371	Fluealp	Zermatt Ophiolite	ZSU	46°00′55.28" N 7°49′27.87" E
	HP-Meta-gabbro	1372	Spitzi Flue	Zermatt Ophiolite	ZSU	46°01′04.37" N 7°49′43.67" E
	HP-Meta-gabbro	1373	Spitzi Flue	Zermatt Ophiolite	ZSU	46°01′01.02" N 7°50′22.47" E
	HP-Meta-gabbro	1374	Blauherd	Zermatt Ophiolite	ZSU	46°00′57.15" N 7°47′08.53" E
	LG-Meta-gabbro	1375	Matterhorn W-Wall	Matterhorn Gabbro	DBN	45°58′56.11" N 7°38′31.34" E
	LG-Meta-gabbro	1376	Matterhorn W-Wall	Matterhorn Gabbro	DBN	45°58′58.54" N 7°38′24.28" E
	LG-Meta-gabbro	1377	Matterhorn W-Wall	Matterhorn Gabbro	DBN	45°58′58.37" N 7°38′34.52" E
	LG-Meta-gabbro	1378	Matterhorn W-Wall	Matterhorn Gabbro	DBN	45°59′02.86" N 7°38′20.54" E
	LG-Meta-gabbro	1379	Matterhorn W-Wall	Matterhorn Gabbro	DBN	45°59′07.14" N 7°38′11.61" E
	LG-Meta-gabbro	1380	Matterhorn W-Wall	Matterhorn Gabbro	DBN	45°58′56.51" N 7°38′39.84" E
	LG-Meta-gabbro	1381	Matterhorn W-Wall	Matterhorn Gabbro	DBN	45°58′38.29" N 7°37′49.09" E
	LG-Meta-gabbro	1382	Matterhorn W-Wall	Matterhorn Gabbro	DBN	45°58′34.40" N 7°37′49.69" E
	HP-Meta-gabbro	875	Allalinhorn	Zermatt Ophiolite	ZSU	46°03′09.57" N 7°55′38.42" E
	HP-Meta-gabbro	876	Allalinhorn	Zermatt Ophiolite	ZSU	46°03′07.76" N 7°55′42.56" E
	HP-Meta-gabbro	877	Allalinhorn	Zermatt Ophiolite	ZSU	46°03′14.22" N 7°55′20.19" E
	HP-Meta-gabbro	879	Allalinhorn	Zermatt Ophiolite	ZSU	46°03′08.68" N 7°55′29.32" E
	HP-Meta-gabbro	880	Allalinhorn	Zermatt Ophiolite	ZSU	46°03′10.23" N 7°55′39.14" E
	HP-Meta-gabbro	881	Allalinhorn	Zermatt Ophiolite	ZSU	46°03′06.98" N 7°55′01.16" E
Meta-basalt	Eclogite	861	Trockener Steg P3030	Theodul glacier unit	TGU	45°57′56.89" N 7°43′01.42" E
	Eclogite	862	Trockener Steg P3030	Theodul glacier unit	TGU	45°57′55.75" N 7°43′02.28" E
	Eclogite	895	Trockener Steg P2931	Theodul glacier unit	TGU	45°58′26.19" N 7°42′22.81" E
	Eclogite	922	Trockener Steg P3002	Theodul glacier unit	TGU	45°58′06.80" N 7°42′45.48" E
	Eclogite	923	Trockener Steg P3002	Theodul glacier unit	TGU	45°58′04.94" N 7°42′49.71" E
	Eclogite	1388	Pfulwe	Zermatt Ophiolite	ZSU	46°00′57.76" N 7°50′08.37" E
	Eclogite	1389	Pfulwe	Zermatt Ophiolite	ZSU	46°00′56.32" N 7°50′04.09" E
	Eclogite	1392	Pfulwe	Zermatt Ophiolite	ZSU	46°00′57.69" N 7°50′08.67" E
	Eclogite	1393	Pfulwe	Zermatt Ophiolite	ZSU	46°00′59.36" N 7°50′40.25" E
	Eclogite	1400	Minugrat*	Bernhard Nappe	SMN	46°10′29.96" N 7°40′34.67" E
	Eclogite	1401	Minugrat	Bernhard Nappe	SMN	46°10′44.02" N 7°40′33.17" E
	Eclogite	1402	Minugrat	Bernhard Nappe	SMN	46°10′44.02" N 7°40′33.17" E
	Eclogite	1403	Minugrat	Bernhard Nappe	SMN	46°10′48.71" N 7°40′28.45" E

HP high pressure, *LG* low grade, *KB#* sample number

* Sample equivalence: 1400 = MRD 92, 1401 = MRD 99a, 1402 = MRD 99b, 1403 = MRD 134 (Rahn, 1991)

This study includes five samples (Table 1) from the TGU (Fig. 1) from the rocky cliff point 3030 near Trockener Steg (Fig. 2a) and from the steep W-slope of point 3002 (see also Figs. 2, 3 in Bucher et al., 2020).

The extrusion age of the basalts is unknown but must be > 295 Ma, the age of the granulite facies metamorphism of the TGU. Weber and Bucher (2015) concluded from their composition data from TGU eclogites that they derive from continental within-plate basalts (WPB) rather than from potential MORB as suggested for the ZSU eclogites. The composition patterns of the TGU eclogites are unique to the Zermatt region and motivated to undertake this study. The TGU eclogite has similarities to eclogites from the Etirol-Levaz slice south of the Zermatt region (Beltrando et al., 2010).

2.2.5 Meta-gabbro of the Dent Blanche Nappe (DBN)

Massive meta-gabbro bodies form a significant part of the DBN (Dal Piaz et al., 1977; Monjoie et al., 2007; Baletti et al., 2012; Manzotti et al., 2017, 2018). The meta-gabbro

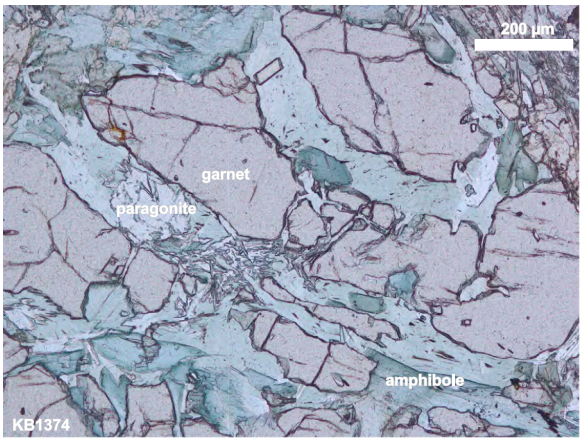

Fig. 3 Photomicrograph of meta-gabbro sample KB1374 from the Pfulwe area (Fig. 1) showing strongly resorbed eclogite facies garnet replaced by glaucophane and barroisitic amphibole during decompression after peak P

masses are bounded by tectonic contacts. This is particularly evident on the west side of the Matterhorn where the top of the massive meta-gabbro wall is marked by a several m thick meta-gabbro mylonite and fine-banded mylonitic gneiss (Figs. 4, 5a). The coarse grained meta-gabbroic rocks are generally internally undeformed. The meta-gabbro masses are exposed at the lower parts of the W- and S-face of the Matterhorn. On the S-side of Matterhorn the contact to the DBN basement gneiss (Arolla gneiss) is a sharp tectonic surface (Fig. 5b). The new geochemical data presented here are from samples of the W-face of Matterhorn (Matterhorn meta-gabbro) and from the outcrops at the NW-foot of Testa del Leone (Table 1). Meta-gabbro masses also build up Mont Collon, gabbro bodies at Alpe Berrio and a layered meta-gabbro complex forming the mountain Dent du Bertol further to the W within the DBN (Bucher et al., 2003; Manzotti et al., 2017; Monjoie et al., 2005; Piaz et al., 1977). The complete lack of internal deformation and the sharp tectonic contact to the deformed Permian granites of the DBN is consistent with a post-Permian tectonic emplacement of the gabbros in the DBN basement. A magmatic age of 284 ± 0.6 Ma has been reported for the Mont Collon meta-gabbros of the DBN (Monjoie et al., 2007).

The dominant Matterhorn meta-gabbro is an metamorphic olivine-gabbro with Opx-coronas around plagioclase (Fig. 6a). The meta-gabbro has a typical uniform grain size of 5 mm and has been variably altered by fluid-rock interaction at very low grade. Whilst igneous plagioclase is well preserved in many samples (Fig. 6a), in other samples only pseudomorphs after feldspar are present with not much plagioclase preserved (Fig. 6b). The alteration products, mainly mica and chlorite saussurite, suggest the alteration occurred at subgreenschist to lower greenschist facies conditions.

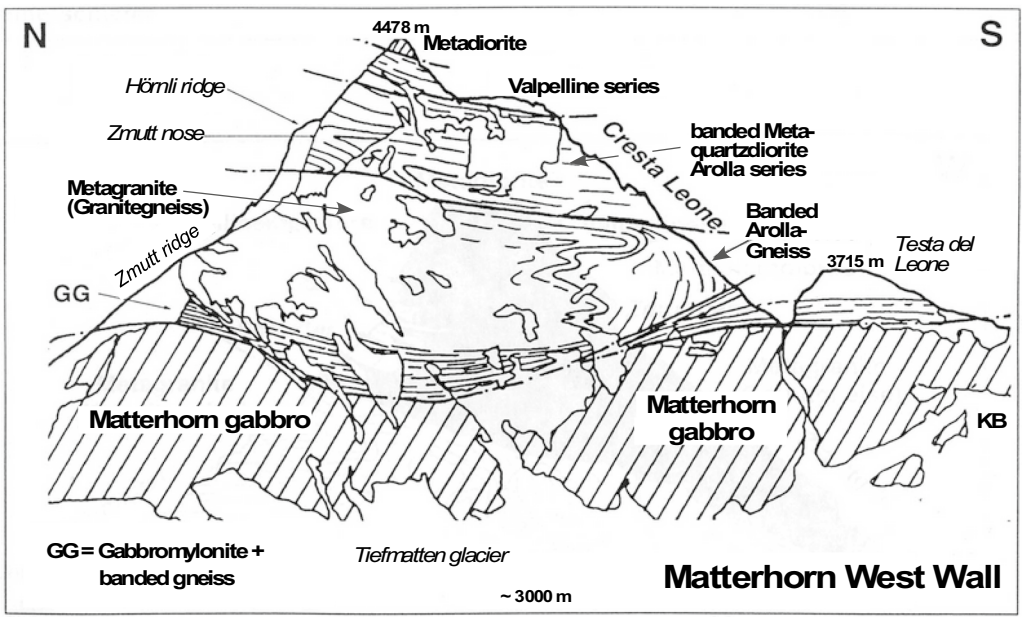

Fig. 4 West wall of Matterhorn (ital. Monte Cervino) with the Permian gabbro above Tiefmatten glacier. The contact to the banded and folded Arolla gneisses of the Dent Blanche nappe above is a zone of gabbromylonite and sheared gneiss (GG)

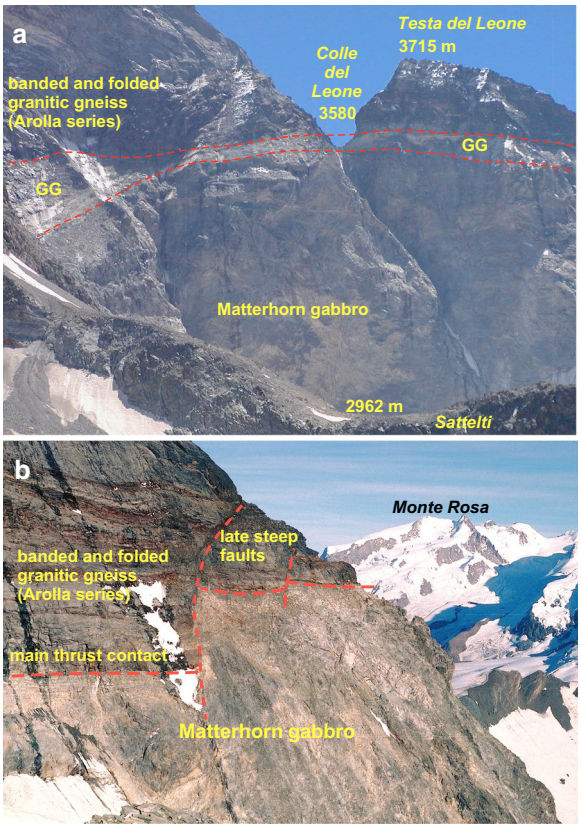

Fig. 5 Field occurrence of Matterhorn gabbro. **a** Massive internally undeformed gabbro body with tectonic contact to the Arolla gneisses marked with locally altered gabbro mylonites (GG). View of the right side of Fig. 4; **b** Top of the Matterhorn gabbro body with sharp tectonic contact to the Arolla gneisses of the Dent Blanche nappe (DBN). View from the ridge above Colle del Leone to the East. In the background Mone Rosa (see Fig. 1)

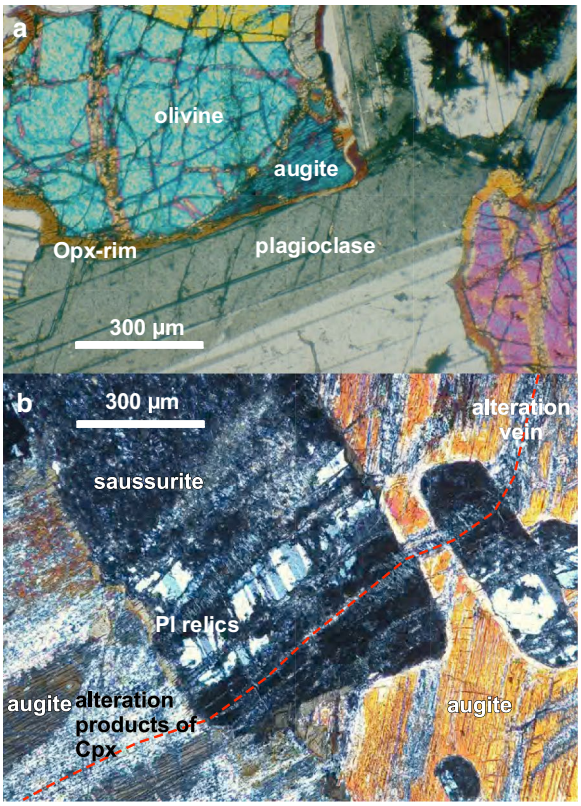

Fig. 6 Photomicrographs of Matterhorn gabbro. **a**) Olivine and augite (Cpx) gabbro with unaltered plagioclase. Thin Opx reaction rims along grain boundaries; **b**) Augite and plagioclase in typical Matterhorn gabbro (KB1381). Pl is strongly altered to saussurite (Ab + Clz), Cpx altered to Chl + Amp by low-temperature reaction with aqueous fluids that migrated along veins (e.g. red dashed line)

2.2.6 Meta-basalt of the Siviez-Mischabel Nappe (SMN)

Mafic meta-volcanic rocks occur as greenschist, amphibolite, eclogite and retro-eclogite in the basement of the SMN. Included in the study are three eclogite samples (Table 1) from the Minugrat in the Turtmann valley collected by Rahn (1991). The eclogites belong to a large outcrop of mafic rocks, mostly amphibolite, mapped as part of the Adlerflüe unit by Marthaler et al. (2008). It is labeled as possibly Proterozoic in age. However, none of the rocks of the Adlerflüe unit have been dated. The age of the eclogite facies metamorphism has been assumed to be pre-alpine and derived P–T estimates for the return-point conditions are 1.2—1.35 GPa and 550—600 °C (Rahn, 1991). The polycyclic basic rocks derive from tholeitic basalts and may have been extruded in a back-arc setting (Eisele et al., 1997).

The SMN eclogites contain the peak assemblage Grt + Omp + Rt ± Ky ± Qz ± Czo. Zoned Grt has Grs-rich cores (Alm 58, Grs 30, Prp 8, Sps 4) and Prp rich rims (Alm 45, Grs 18, Prp 36, Grs 1) (Rahn, 1991). A Domino/Theriak model (see Sect. 2 Methods below) for the eclogite sample JSE-5 suggests, however, more extreme conditions for equilibration of the Grt + Omp + Ms + Ky + Qz assemblage. The Grt rims may have grown at $T > 700$ °C and $P \sim 2.5$ GPa. Garnet cores suggest $T < 500$ °C and $P \sim 2$ GPa. The assemblage at the Grt core formation contained Lws, Pg, Qz, Gln in addition to Grt and Omp, consistent with reported Lws pseudomorphs and relic Na-amphibole (Rahn, 1991).

3 Methods

Whole rock analysis was performed by standard X-ray fluorescence (XRF) techniques at the University of Freiburg, Germany, using a Philips PW 2404 spectrometer. Pressed powder and Li-borate fused glass discs were prepared to measure contents of trace and major elements, respectively. Raw data were processed with the standard XR-55 software of Philips. Relative standard deviations are < 1 and < 4% for major and trace elements,

respectively. Loss on ignition was determined by heating at 1,100 °C for 2 h.

Rare earth elements (REE) and trace element analysis were performed by sodium peroxide fusion ICP AES at SGS Minerals Services in Lakefield, Ontario Canada.

P–T conditions during garnet growth for the SMN sample JSE-5 (Eisele et al., 1997) have been deduced from assemblage stability diagrams and assemblage models at *P–T* using Theriak/Domino software of de Capitani and Petrakakis (2010), and thermodynamic data from Berman (1988) (JUN92 data and updates). The thermodynamics of garnet solutions, omphacite and white mica follow the models of Berman (1988), Meyre et al. (1997) and Keller et al. (2005), respectively.

4 Results: the composition of the basic rocks

35 rock samples (Table 1) have been analyzed for major elements, trace elements and REE (Additional file 1: Tables S1–S4). The rocks include 21 meta-gabbro and 14 meta-basalt samples from the larger Zermatt region. The meta-gabbros comprise 7 samples from 3 different localities in the ZSU near Zermatt (Fig. 1), 6 samples from the Allalin meta-gabbro also belonging to the ZSU and 8 samples from Matterhorn meta-gabbro associated with the DBN from the west wall of Matterhorn (Figs. 4, 5). The meta-basalts are exclusively samples of eclogite including 5 samples from the TGU, 5 eclogites from the ZSU and 4 samples from the SMN. Greenschists, amphibolites and other meta-basaltic rocks have not been included in the study in that way avoiding the additional complexity added by further fluid-rock rock alteration episodes.

The three groups of meta-volcanic samples show distinct differences in composition (Fig. 7a). Eclogites from the TGU and those from the SMN (Minugrat samples) plot closely together in the basalt field. The ZSU samples, however, are rich in total alkalis and silica and plot strictly into the field of basaltic trachyandesite.

The meta-gabbros of the continental Dent Blanche nappe and the ophiolitic Zermatt-Saas Unit are Ol-normative. However, the Matterhorn meta-gabbro from the DBN contains normative hypersthene in contrast to the ophiolitic meta-gabbro indicating deeper crystallization depth at higher pressure in agreement with a continental origin of the DBN gabbros (Schmidt et al., 2016; Shamberger & Hammer, 2006). The total alkalis versus silica (TAS) diagram (Fig. 7b) shows that all meta-gabbro samples fall into field of normal tholeitic gabbro with the exception of three samples from the ZSU (1369, 1370, 1393). The ZSU meta-gabbro samples, excluding the Allalin meta-gabbro, form a linear array of points and increase in alkalis and silica from the gabbro field to the field of monzo-diorites. The Matterhorn meta-gabbros

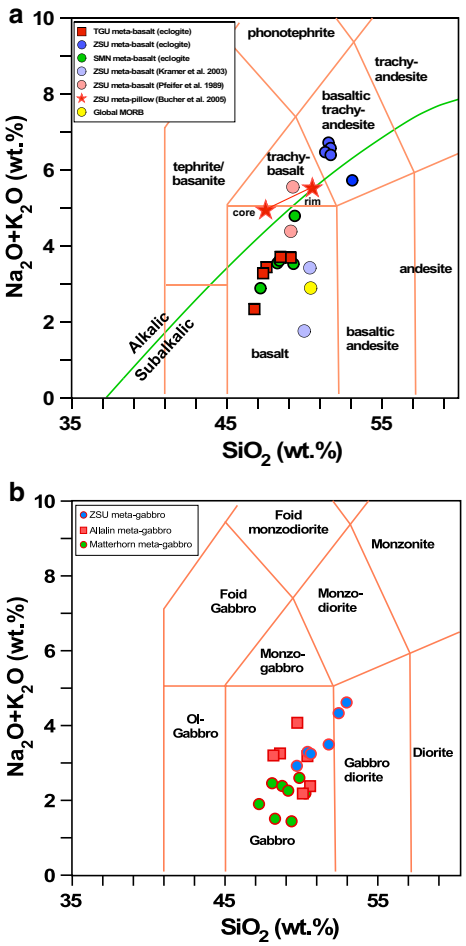

Fig. 7 Total alkalis vs. silica diagram (TAS diagram) for **a** metamorphic basalt (eclogite) and **b** meta-gabbro from the Zermatt region. Definition of fields from Le Maitre et al. (2002) and Le Bas et al. (1986). Alkalic-Subalkalic boundary after Irvine and Baragar (1971). Yellow point = Global MORB (Arevalo & McDonough, 2010)

from the DBN overlap with the unaltered samples from the Allalin meta-gabbro of the ZSU (875, 876).

Gabbro (meta-gabbro) differs clearly from eclogite (meta-basalt) with respect to X_{Mg} or Mg-number (Fig. 8). The X_{Mg} of the meta-gabbro samples is close to 0.82 on average. The X_{Mg} of the eclogites range from 0.48 to 0.62. The average silica content of the rocks excluding the ZSU samples is 49 wt.% SiO_2. The ZSU samples are more silica-rich and contain about 51.5 wt.% SiO_2 on average (blue symbols on Fig. 8). The eclogite sample 1393 from the ZSU (Pfulwe area, Table 1) with a high X_{Mg} and SiO_2 is probably of gabbroic rather than basaltic origin. Strongly deformed meta-gabbro may be difficult to recognize and textural evidence can be weak and ambiguous at some outcrops. Also on the AFM diagram (Fig. 9a) all meta-gabbros cluster in an Mg-rich field,

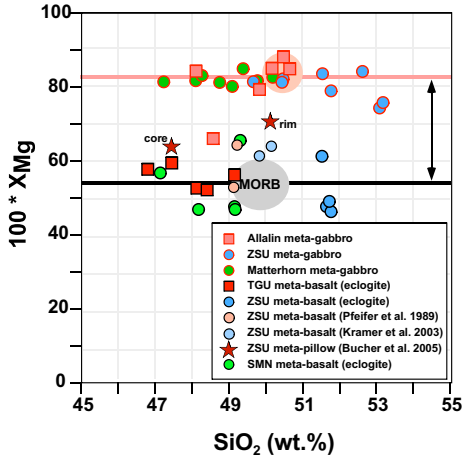

Fig. 8 Major element composition of mafic rocks depicted on an X_{Mg} vs. silica diagram. Meta-gabbro with red-rimmed symbols, meta-basalt (eclogite) with black-rimmed symbols. Pink field = least altered ZSU meta-gabbro. Gray shaded field = MORB. Average #Mg gabbro = 82, basalt = 54: Arrow = Δ#Mg (gabbro—basalt) = 28

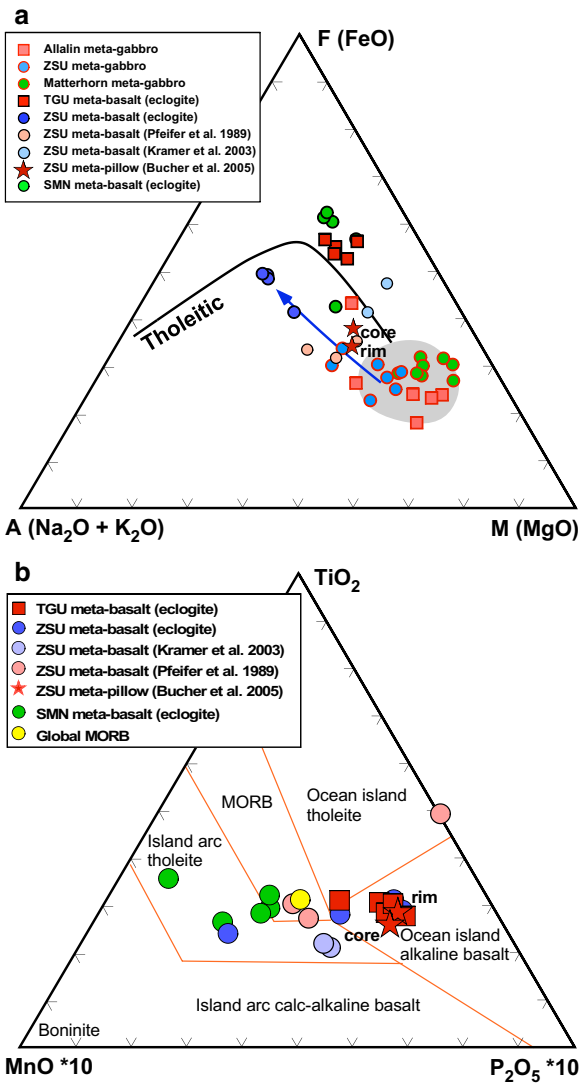

Fig. 9 **a** AFM diagram with tholeitic trend from Kuno (1969). Gray shaded field for meta-gabbro. Blue arrow = trend of ZSU basalt and gabbro resulting from metasomatic alteration; **b** Ti-Mn-P diagram (Mullen, 1983). Yellow symbol = global MORB

while the eclogitic meta-volcanics follow a tholeitic evolution trend. The ZSU eclogites define a modified trend starting from the ZSU meta-gabbros (blue symbols and blue arrow on Fig. 9a). On the Mullen diagram (Fig. 9b) two ZSU eclogites from Pfeifer et al. (1989) plot close to global MORB (and one sample lacks MnO). However, the group of all ZSU eclogites including the meta-pillow samples follow a trend from MORB to the Mn-poor side of the diagram. The TGU eclogites are located in the OIAB field, whereas the SMN eclogites fall into the MORB or IAT fields.

In a trace element (Ti-Zr-Y) discrimination diagram (Pearce & Cann, 1973), all TGU eclogites are located in WPB field characteristic for continental rift basalts (Fig. 10a). All SMN eclogites are central in the field of MORB + CAB. The ZSU eclogites cover a very wide range of Ti-Zr-Y compositions. The significance of this Ti-Zr-Y distribution is discussed in some detail in the discussion section below.

The discrimination diagram using the trace elements Zr–Nb-Y (Meschede, 1986; Fig. 10b) shows that all TGU meta-basalts cluster in the field of within plate basalts in agreement with the samples of Weber and Bucher (2015). The SMN eclogites group in the IAB and N-MORB field. The ZSU eclogites show a wide range of compositions similar to the pattern of the Zr-Y–Ti distribution (Fig. 10a) (see discussion section below).

The primitive mantle (PM) normalized trace element concentrations show distinct differences between basalts (Fig. 11a) and gabbros (Fig. 11b). The total of trace elements is generally higher in basalts compared with gabbros. Most meta-basalts show a marked depletion in Sr relative to PM, the meta-gabbros a very strong enrichment in Sr. The meta-volcanics show a weak depletion in Eu, the meta-gabbros a distinct Eu enrichment. The SMN eclogites follow a N-MORB pattern except for the elements to the left of Nb; the ZSU eclogites are closer to the E-MORB trend. The TGU eclogites clearly follow a trend typical of continental rift basalts (Fig. 11a). However, TGU and SMN eclogites show Ba, Rb and Cs concentration patterns that are quite different from the MORB and

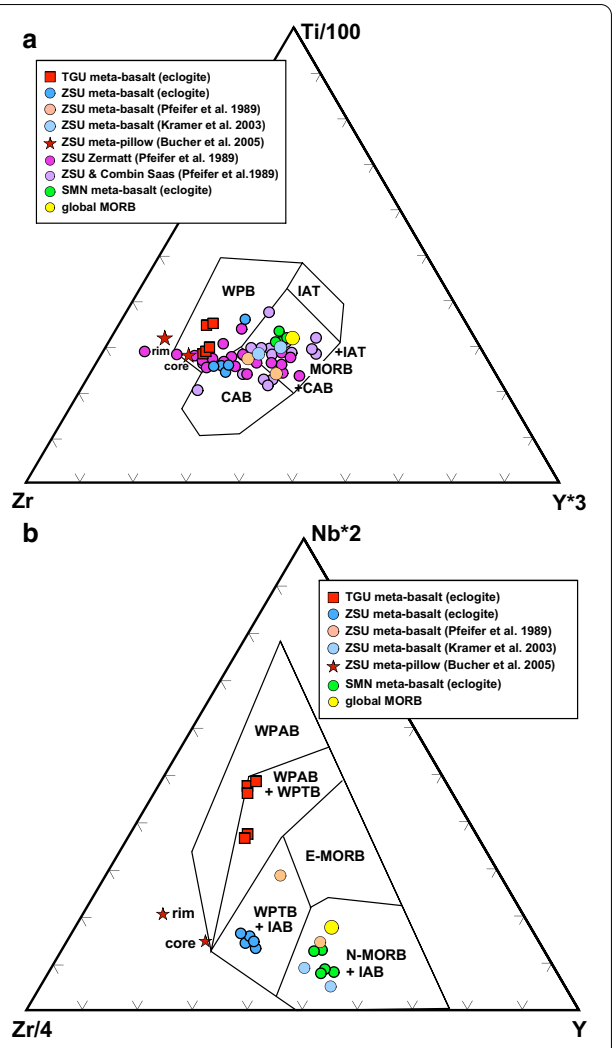

Fig. 10 **a** Zr-Ti-Y diagram with fields for basaltic rocks from Pearce and Cann (1973). WPB within plate basalts, IAT island arc tholeites, MORB mid-ocean ridge basalt, CAB continental margin arc basalts. ZSU meta-basalt from Pfeifer et al. (1989): pink symbol 2 analyses from Table 2, ZSU Zermatt data from Fig. 5, ZSU & Combin Saas data from Fig. 5. Global MORB from Arevalo and McDonough (2010). **b** Nb-Zr-Y discrimination diagram (after Meschede, 1986). WPAB within plate alkali basalt, WPTB within plate tholeitic basalt, E-MORB enriched mid-ocean ridge basalt, N-NORB normal mid-ocean ridge basalt, IAB island arc basalt

OIB + CAB trends. The SMN eclogites the elements from U to Cs show a unique massive enrichment relative to the average N-MORB. Cs is two orders of magnitude higher than in N-MORB. U shows a marked enrichment for all SMN samples. Meta-gabbro trace element compositions run parallel for elements from Nb to Yb, the elements to the left of Nb do not show a simple pattern and several elements in the ZSU gabbros were below detection limit.

The chondrite normalized REE patterns of meta-basalts (Fig. 12a) and meta-gabbros (Fig. 12b) show clearly separated and distinct trends for the rocks from the three different tectonic units. The TGU rocks follow an OIB or CAB pattern, ZSU eclogite is above the E-MORB and SMN eclogite along the E-MORB trend. Meta-gabbro is generally slightly lower in REE than eclogite and Matterhorn meta-gabbro slightly higher than ZSU meta-gabbro with the exception for a few outliers. There is a distinct Eu enrichment in all meta-gabbro samples.

5 Discussion and interpretation of data

The metamorphic basalts and gabbros of the Zermatt region display distinct and characteristic composition patterns related to the tectonic setting of the original basic magmas. The composition of the rocks was modified by post-magmatic processes including seafloor alteration of basalt, polycyclic and poly-phase metamorphism, interaction with fluids during subduction to 50–90 km depth, deformation-assisted hydration and subsequent dehydration.

Any reconstruction of the compositional characteristics of the originally basic igneous rocks must first detect and characterize the post-magmatic modification of the meta-basalts and meta-gabbros.

5.1 Characterization of chemical alteration of basalts and gabbros

5.1.1 ZSU ophiolites

The ZSU meta-basalts suffered extensive modification by post-magmatic processes. Extensive alteration of the ZSU meta-basalts occurred by interaction with seawater at the ocean floor. This is suggested by the composition patterns of ZSU meta-basalts (Figs. 7, 8, 9, 10) and the compositional zoning of pillows documented for meta-basalt of the Pfulwe area E of Zermatt (Bucher et al. 2005). Spillitization is a possible process altering basalts at the seafloor. It produces mainly chlorite-epidote-calcite greenstone from the primary basalt minerals and glass. Albite can also occur as an abundant alteration product. Spillitization tends to drastically increase Mg of the altered basalt and it removes Ca. (e.g. Hernández-Uribe et al., 2020; Seyfried et al. 1978).

The following Al-balanced model reaction illustrates the spillitization of pillow basalt using a slightly simplified composition of global MORB (Arevalo & McDonough, 2010):

$$8\,Na_2Mg_4Fe_3Ca_5Al_7Si_{19}O_{61.5}(\mathrm{MORB}) + 39\,MgCl_2 + 2\,NaCl + 76\,H_2O = 19\left(Mg_{0.57}Fe_{0.43}\right)_5Al_2Si_3O_{10}(OH)_8 + 18\,NaAlSi_3O_8 + 41\,SiO_{2aq} + 40\,CaCl_2 \quad (1a)$$

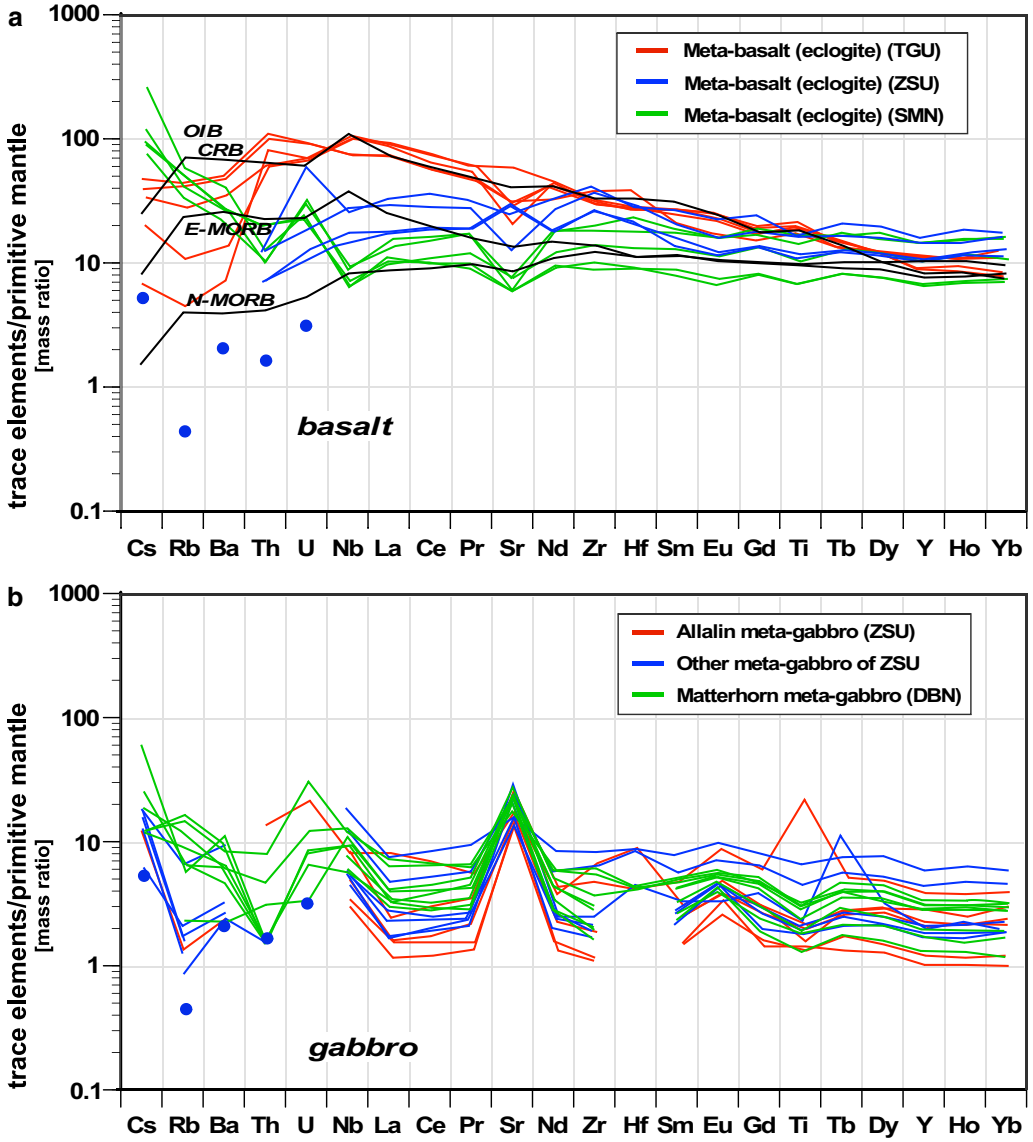

Fig. 11 Trace element composition of metamorphic mafic rocks normalized to primitive mantle. Normalizing factors are from Lyubetskaya and Korenaga (2007). N-MORB, E-MORB, and OIB (CAB) reference patterns are from Sun and McDonough (1989). OIB ocean island basalts. Blue dots = detection limit. **a** Meta-basalt (eclogite); **b** Meta-gabbro

or in a simplified version:

$$\text{MORB} + \text{MgCl}_2 + \text{NaCl} + \text{H}_2\text{O} = \text{Chl} + \text{Ab} + \text{SiO}_{2\text{aq}} + \text{CaCl}_2 \quad (1b)$$

The produced greenstone is enriched in Mg and depleted in Ca and Si. The ZSU eclogites show a generally increased total of alkalis, magnesium and silica (Fig. 7). This could indicate that the basalts were altered by processes other than spillitization.

An alternative potentially possible process involves basaltic glass as reactant and chlorite as product in addition to mica (clay). A typical sink for Ca in oceanic basalt alteration is a vast variety of zeolites (e.g. Weisenberger et al. 2020). Although Al-conservation is certainly not strictly followed by hydrothermal alteration processes the element is generally captured by the product minerals. The hydration of MORB glass typically produces chlorite and zeolite in addition to albite or clay. The effects of MORB hydration can be illustrated by

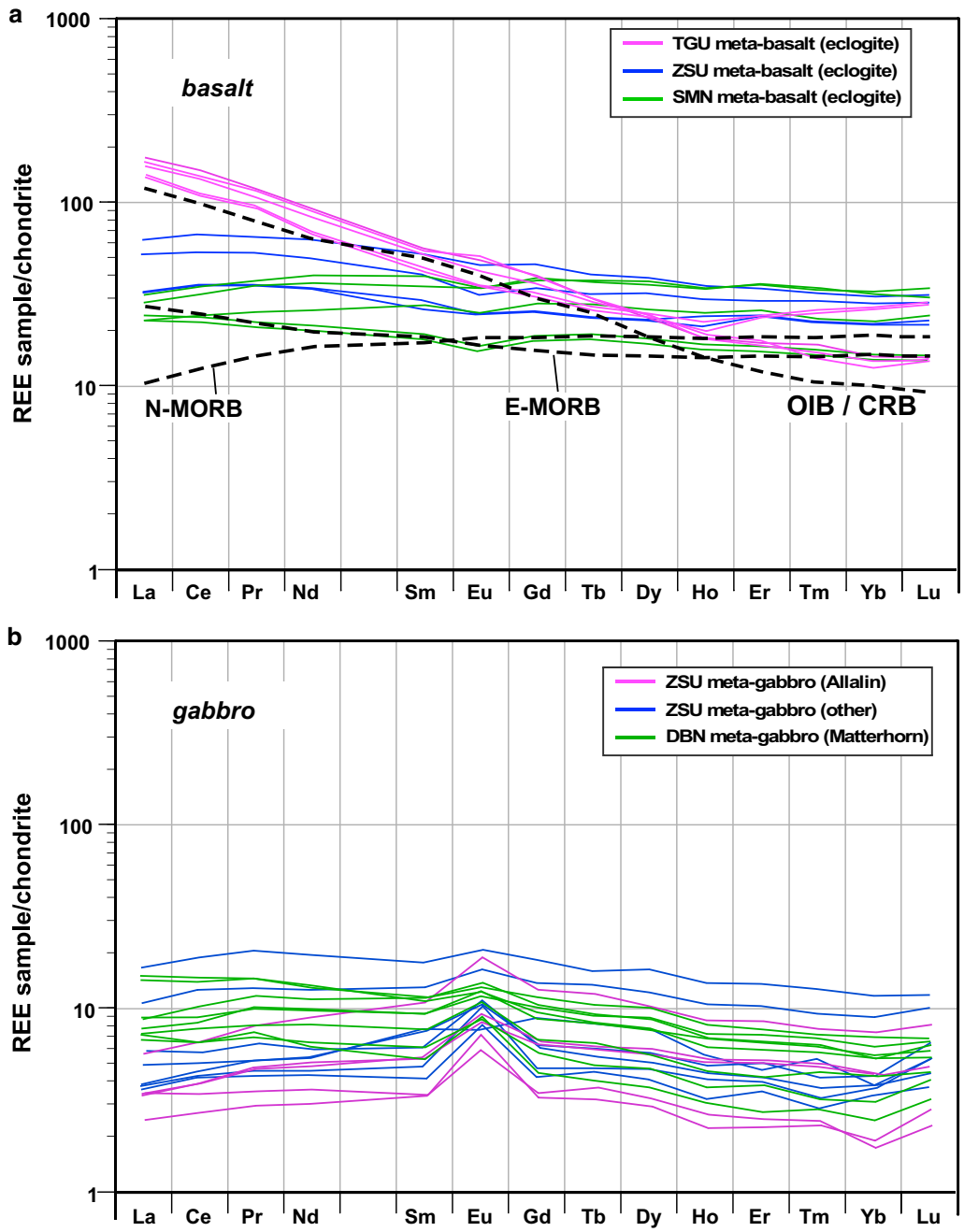

Fig. 12 Chondrite normalized REE composition of meta-basic rocks from the Zermatt region. Normalizing factors are from McDonough and Sun (1995). **a** Meta-basalt (eclogite). N-MORB, E-MORB, and ocean island basalt (OIB) reference patterns are from Sun and McDonough (1989); **b** Meta-gabbro

the following reaction using the same slightly simplified composition of global MORB as in reaction 1 (Arevalo & McDonough, 2010):

$$\begin{aligned} &Na_2Mg_4Fe_3Ca_5Al_7Si_{19}O_{61.5}(\text{MORB}) + 7.8\ \text{NaCl} \\ &+ 10\ H_2O = 1.4\left(Mg_{0.57}Fe_{0.43}\right)_5Al_2Si_3O_{10}(OH)_8 \\ &+ 1.1\ CaAl_2Si_7O_{18} * 6H_2O + 2\ NaAlSi_3O_8 \\ &+ 1\ SiO_{2aq} + 3.9\ CaCl_2 \end{aligned} \tag{2a}$$

or in the simplified version without stoichiometric coefficients:

$$\mathrm{MORB} + \mathrm{NaCl} + \mathrm{H_2O} = \mathrm{Chl} + \mathrm{Heu} + \mathrm{Ab} + \mathrm{SiO_{2aq}} + \mathrm{CaCl_2} \quad (2b)$$

Reaction (2) illustrates the transformation of bulk MORB or MORB glass to low grade basic rocks with the Ab—Heu—Chl assemblage typical of low-grade zeolite facies meta-basalts by the interaction with seawater. The model reaction (2) uses pure Ca-heulandite as product zeolite. Heulandite and other Ca–zeolites in altered basalt typically also contain some Na (Weisenberger & Selbek, 2009; Weisenberger et al., 2020). Some of this Na present in zeolite may be of late groundwater origin, however (Bucher & Weisenberger, 2013). Reaction (2) releases SiO_2 to the hydrothermal fluid from where it precipitates as amorphous silica if the fluid reaches the surface as the many Icelandic occurrences testify. The reaction (2), which may be called zeolitization, stands for a reasonable process substituting spillitization (R1). It is a model for the hydrothermal alteration of massive basaltic rocks rather than pillow lava, which undergoes spillitization by reaction (1).

Zeolitization (R2) during very low grade alteration of basic igneous rocks including basaltic glass generally increases the alkalis of the original rock and produces an altered rock with lower SiO_2 and CaO in the bulk composition.

During high-*P* low-*T* metamorphism associated with Alpine subduction the Zermatt-Saas ophiolites reacted with subduction zone fluids (Bucher & Grapes, 2009). In the Allalin meta-gabbro the hydrous mineral zoisite formed along the decent path together with Ky, Jd and Qz because fracture permeability has been created by brittle deformation associated with subduction. Later at maximum *P* olivine was completely hydrated to talc and chloritoid. Finally glaucophane and phengite very late paragonite and margarite in addition to rare chlorite formed along the ascent path associated locally with ductile deformation. Stepwise fluid-rock reactions resulted in a product rock with more than 10 different hydrous minerals from an initially dry gabbro containing plagioclase, augite and olivine but no hydrous minerals. Consequently the composition difference between the rarely preserved original gabbro (sample 876, Additional file 1: Table S1) and its maximum hydrated version (sample 881, Additional file 1: Table S1) document the total effect of meta-gabbro interaction with subduction zone fluids. Based on an Al-conserved reference frame, it is evident that the interaction with subduction zone fluids massively removed silica and a large amount of CaO and MgO from the original gabbro and added Na_2O and volatile components. The trace element data (S2) show that the rock significantly lost Sr and gained Zr. Other trace element data from the Allalin meta-gabbro (Bucher & Grapes, 2009) show that the combined effect of fluid-rock reaction in the subduction zone is a substantial loss of Cr, Cu, V, Ni, and Co. The REE data (S3) show that gains and losses of rare earth elements are relatively small. The rock altered by subduction zone fluids gained some Ce and also La and small amounts of Nd and Sm. Very small or no losses of heavy REE contrast with the gains in light REE. The effects of subduction zone alteration of gabbroic igneous rocks are very similar to the hydrothermal alteration of basaltic glass (model reaction 2). In summary: The Allalin meta-gabbro experienced no alteration prior to the Alpine subduction related high-*P* metamorphism and the derived losses of silica, Mg and Ca and gains of Na exclusively relate to the high-*P* fluid-rock reactions.

The basaltic volcanic rocks of the Zermatt-Saas ophiolite show locally preserved pillow structures (Bearth, 1967; Bucher et al., 2005). However, no unaltered basaltic rocks have been found anywhere in the Zermatt-Saas region. The meta-basaltic rocks show clear compositional differences between pillow cores, pillow rims and inter-pillow material (Bucher et al., 2005). Pillow cores are eclogite, pillow rims consist of glaucophanite and inter-pillow material is a chlorite-rich Gln-Pg rock. Paragonite and glaucophane together with chloritoid are texturally late minerals in eclogite. The eclogite cores also contain abundant ankeritic/dolomitic carbonate. Again using an Al-balanced reference frame, the rims gained Si, Mg, Na and lost Ca, Fe, CO_2. The lost components mostly originate from removal of carbonate. Mg and Na increase may indicate interaction of basalt with seawater. However the Si-increase in the altered rims of the pillows requires a mechanism different from spillitization (reaction 1) or zeolitization (reaction 2). A potential process generating the observed composition pattern of pillow basalt is:

$$2\,\mathrm{Na_2Mg_4Fe_3Ca_5Al_7Si_{19}O_{61.5}(MORB)} + 11\,\mathrm{MgCl_2} + 20\,\mathrm{H_2O} = 5\left(\mathrm{Mg_{0.57}Fe_{0.43}}\right)_5\mathrm{Al_2Si_3O_{10}(OH)_8} + 4\,\mathrm{NaAlSi_3O_8} + 11\,\mathrm{SiO_{2aq}} + 2\,\mathrm{NaCl} + 11\,\mathrm{CaCl_2} \quad (3a)$$

or in a simplified version:

$$\mathrm{MORB} + \mathrm{MgCl_2} + \mathrm{H_2O} = \mathrm{Chl} + \mathrm{Ab} + \mathrm{SiO_{2aq}} + \mathrm{CaCl_2} \quad (3b)$$

Alternatively the compositional zoning of the pillow basalts could be the result of interaction of the intact basalt with subduction zone fluids. We prefer the reaction with seawater because the compositional feature is clearly tied to the pillow structure. The pillow core is enriched in Mg, Na and CO_2 compared with Mid-Atlantic Ridge MORB (Carmichael et al. 1974) and it lost Si,

Fe, and Ca. These properties support the interpretation of active seawater alteration of the pillow basalts by reactions similar to the model reaction (3) prior to Alpine metamorphism.

5.1.2 Matterhorn meta-gabbro

All samples from Matterhorn meta-gabbro (DBN) show effects of low-grade alteration to various extents (Fig. 6). The Al-balanced reaction (4) describes the replacement of the anorthite component in igneous labradoritic plagioclase by albite through the interaction with continental crustal Na-Ca–Cl-type fluids (Stober & Bucher, 2005a, 2005b):

$$CaAl_2Si_2O_8 + 2\,NaCl + 4\,SiO_{2aq} = 2NaAlSi_3O_8 + CaCl_2 \quad (4)$$

Reaction 4 is a model for albitization of basic igneous rocks. Albitization is a common and widespread process at low grade metamorphic conditions (e.g. Putnis & Austerheim, 2020).

The anorthite component of labradorite can also be replaced by clinozoisite/epidote. Epidote is then part of the Ep-Ab pseudomorphs replacing plagioclase. Altered Matterhorn meta-gabbro typically contains calcite and chlorite in addition to albite and epidote. The textures suggest that labradorite reacts with a CO_2 bearing fluid:

$$4(NaAlSi_3O_8 - CaAl_2Si_2O_8) + 1\,CO_2 + 1\,H_2O = 2Ca_2Al_3Si_3O_{12}(OH) + 3NaAlSi_3O_8 + CaCO_3 \quad (5)$$

Reaction (5) describes the full conversion of labradoritic plagioclase to Clz(Ep) and Ab. The assemblage is known as saussurite (Fig. 6). It has no effect on the position of the Matterhorn meta-gabbros on the TAS diagram (Fig. 7). The co-produced calcite is often found in small veinlets or in veins with chlorite and/or quartz. Chlorite and epidote/clinozoisite form at low-T from the alteration of augite (Fig. 6).

5.2 Significance of compositional variation of basic igneous rocks

The distinct and prominent difference of X_{Mg} between gabbro and basalt (Fig. 8) is considered a magmatic feature ($\Delta X_{Mg} \sim 0.28$). The early Fe–Mg silicates crystallizing in gabbro magma chambers at liquidus conditions tend to have a high X_{Mg} (Carmichael et al., 1974). The gap between ZSU meta-gabbro and ZSU basalt is consistent with the absence of dyke systems characteristic of ophiolites in the Zermatt-Saas Unit. The conspicuous absence of sheeted dykes in the ZSU has been recognized in many field studies and is not a bias of our relatively few samples.

A consequence of the post-magmatic alteration of the ZSU rocks is that the eclogites evolve along an unusual trend in AFM space from the ZSU meta-gabbro (blue arrow Fig. 9a). This trend is consistent with the proposed zeolitization reaction (2) that increases Na and produces zeolite—chlorite greenstone from basalt (Fig. 7). All other rocks, including the massive Allalin meta-gabbro follow a typical tholeitic liquid line of descent where gabbro and basalt are related through the $FeMg_{-1}$ exchange (Villiger et al., 2004).

The Mullen diagram (Fig. 9b) shows the relative proportions of the minor elements Ti, Mn and P. The TGU eclogite samples cluster together in the field of OIB (or CRB), whereas the eclogites from SMN fall into the MORB or IAT fields due to their higher relative MnO content. The Mullen diagram appears not to be particularly helpful for deciphering the geodynamic background of the ZSU rocks. However, it suggests that the eclogites of the ZSU developed from primary basalt by loss of MnO (Fig. 9b). This is remarkable because the same transition is accompanied by a relative gain in FeO (Fig. 9a). Our preferred interpretation of the data distribution is that $FeMg_{-1}$ is an igneous process but that the loss of MnO results from low-temperature alteration of basalt. MnO can be lost from the basalt by the reaction of igneous augite with hot fluids, e.g. heated seawater or crustal fluids.

$$0.5Mn_2Si_2O_6 + 2Ca(Mg,Fe)Si_2O_6 + 1.5(Mg,Fe)_2Si_2O_6 + 2HCl + H_2O = Ca_2(Mg,Fe)_5Si_8O_{22}(OH)_2 + MnCl_2 \quad (6)$$

Reaction (6) converts augite to amphibole and Mn from the primary kanoite component is lost to the fluid and may possibly precipitate as Mn-nodules or Mn-crusts on the seafloor. The ZSU eclogites and greenstones are accompanied by meta-cherts that locally contain pink layers and patches rich in Mn-silicates, mostly piemontite and spessartite (Bearth & Schwander, 1981). The TGU eclogites probably did not lose Mn by an ocean-floor process described by reaction (6). The eclogites from SMN have not been altered by such a process and their assignment to the MORB and IAT fields (Fig. 9b) may have geodynamic significance.

5.3 Trace elements: geodynamic background of mafic rocks and post-magmatic alteration

The relative amounts of some trace elements portray the geological background of the samples and the effects of later alteration particularly well (Fig. 10). The distribution of Ti, Zr and Y shows that the TGU eclogites form a distinct group within the fields of within plate basalts (Fig. 10a) and within plate tholeites (Fig. 10b). The SMN eclogites form a distinct group in the MORB field. Data

reported for the ZSU eclogites scatter over a wide range (Fig. 10a). Our own data from the Pfulwe eclogites cluster in the CAB field. Two data points from Pfeifer et al. (1989) (representative analyses their Table 2) are at the boundary of the CAB and MORB field. Two sets of data points have been taken from the Fig. 5 of Pfeifer et al. (1989). These two sets scatter over a very wide range. The set with the samples from the Saas valley and the Combin unit has its statistical center in the MORB field; the set from the Zermatt area scatters over a very wide range of Zr/Y ratios (Fig. 10a). Our pillow basalt sample (Bucher et al. 2005) is low in Y and fits into the general ZSU array. Two samples from Kramer et al. (2003) are located in the MORB field. The very large variation in Ti-Zr-Y reported for the ZSU meta-basalts is most likely related to post-magmatic alteration of the basalts by fluid-rock interaction at the sea floor, the shallow oceanic crust and later during the various metamorphic/metasomatic alteration episodes. The data distribution shown on Fig. 10a suggests that the main variation occurs along the ZrY_{-1} exchange vector and that Ti remained mostly constant (at about 30% Ti/100). Assuming an original composition for the ZSU close to MORB (34 Zr—34 Y*3—32 Ti/100) the ZSU rocks lost Y and gained Zr. The most extremely altered greenstone contains 64 Zr—6 Y*3—30 Ti/100. It is evident that Zr and Y were mobile elements during ZSU basalt alteration and that the distribution of the data points does not have significance for the geodynamic origin of the original basalts. This finding is in contrast to common belief that Zr and Y behave as immobile elements (e.g. Floyd & Winchester, 1978). However, it supports the preferential enrichment of Y relative to Zr in Cl-solutions experimentally reacted with eclogites under eclogite facies conditions (Tsay et al., 2017). The ZSU data suggest that Y can be considerably leached from meta-basalt during HP metamorphism.

The primitive mantle normalized trace element patterns (Fig. 11) show that none of the basic rocks from the Zermatt region strictly follow MORB arrays (Gale et al., 2013). From Nb to Yb the TGU eclogites follow a distinct OIB/CRB trend; the ZSU and SMN eclogites show similar MORB-type trends. However, all eclogites show a distinct Sr-depletion except for one sample from the ZSU. The Sr depletion is counterbalanced by the Sr-enrichment of the meta-gabbros indicating that it could be a primary feature of the rocks. The Sr-behavior can be explained by Sr-fractionation into Pl in cumulate gabbros leaving Sr-depleted basaltic liquids. However, the basalt alteration reactions derived for the ZSU rocks (R1–R3) release Ca from the rock to the fluid. Meta-basalts that experienced massive hydrothermal Ca-depletion definitely also have lost Sr. Thus the Sr-depletion of the eclogites reflects post-magmatic fluid-rock reactions. Furthermore, the patterns document a clear Zr enrichment and a subtle but distinct Y depletion relative to the MORB arrays. This is the same ZrY_{-1} exchange that has been described and discussed above in the context of Zr-Y–Ti variations (Fig. 10a). The mobility of the HFSE elements Zr and Y is probably related to fluid-rock interaction during subduction-related HP metamorphism. If the alteration related Sr, Zr and Y anomalies are smoothed, both the ZSU and the SMN eclogites follow MORB type trends for elements Nb to Yb.

The behavior of the elements from Cs to U is distinctively different from all reference patterns (Fig. 11) for all sample groups. The SMN eclogites from Minugrat show a consistent U enrichment, which can be related to local nearby hydrothermal Co–Ni-U deposits (Ansermet, 2012). The SMN eclogites also show dramatically increasing element concentrations from Ba to Rb and Cs. The origin of this pattern could be related to the interaction with the same crustal fluids that generated to Co–Ni-U deposits. The TGU eclogites follow a OIB-CRB pattern from Th to Yb but show an unusual depletion in Ba, very low Rb and a curious prominent Cs increase from low Rb, which is in sharp contrast to a MORB reference pattern for basalts. The pattern for the mobile trace elements (Fig. 11) correlates with a large K variation of the TGU rocks (Fig. 13). The meta-basalts that have been least affected by alteration have low Ba/Rb and high K, eclogites affected by alteration processes gradually decrease in K and increase in Ba/Rb because Rb decreases with K. The ZSU eclogites with very low Cs-Rb-Ba may have lost these mobile trace elements during interaction with hydrothermal oceanic or with subduction zone fluids.

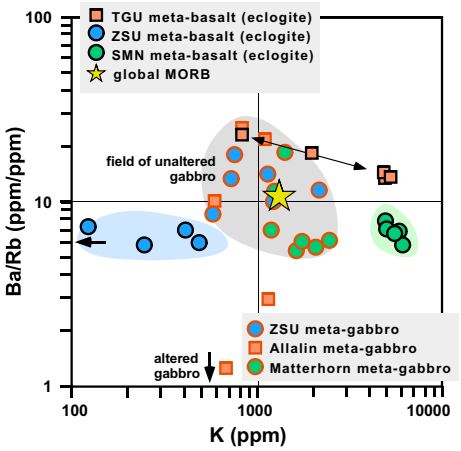

Fig. 13 Ba/Rb versus K diagram (after Bebout, 2007). Gray field = weakly altered gabbro, blue field = ZSU eclogites, Green field = SMN eclogites, TGU eclogites with K-Rb infiltration. Yellow star = Global MORB from Arevalo and McDonough (2010)

The process also removed K in agreement with very low Rb and Ba.

All meta-gabbro trace element patterns show a drastic positive Sr-anomaly. The PM-normalized Sr increases by an order of magnitude. The very pronounced Sr enrichment has also been reported from the DBN meta-gabbros of the south wall of the Matterhorn (Cervino samples of Manzotti et al., 2017). The meta-gabbros show a pronounced enrichment in Cs and less prominent in Ba. U-Th concentrations remain below the detection limit for all ZSU samples including Allalin meta-gabbro. The trace element patterns (Fig. 11) of the meta-gabbros are relatively similar and consequently do not discriminate the different geotectonic origin of the DBN and the ZSU gabbros.

However, the average chondrite normalized $(Ce/Yb)_N$ ratio of 1.32 for the ZSU meta-gabbro is very close to the corresponding ratio of 1.31 for the Allalin meta-gabbro samples suggesting a related origin for the two groups of meta-gabbro samples. The Matterhorn meta-gabbros have a clearly different average $(Ce/Yb)_N$ ratio of 2.04 in agreement with its different geological history and origin. The average $(Ce/Yb)_N$ ratio of the ZSU meta-basalts is 1.77 and for the SMN meta-basalts from Minugrat 1.25. The TGU samples have a drastically different $(Ce/Yb)_N$ ratio of 7.71 in agreement with other trace element concentration (Figs. 10, 11) suggesting a CRB or WPB origin of the TGU meta-basalts.

5.4 Rare earth element composition of meta-basites of the Zermatt region

The chondrite normalized REE patterns of the ZSU eclogites (Fig. 12a) closely follow an N-MORB pattern for the heavy REE. The ZSU eclogites have distinctly higher light REE concentrations but they display the same curved pattern like N-MORB. Two samples from the Minugrat (SMN) very closely follow an E-MORB pattern and three samples are similar to the patterns of the ZSU eclogites. The TGU eclogites very closely follow a OIB/CRB pattern for the elements La through Ho. Three samples continue to follow the same pattern to Lu whilst two samples show increasing concentrations of the elements Er to Lu. We prefer to interpret the TGU meta-basalts as continental rift basalts (CRB/CAB) or within-plate basalts (WPB) (see also Figs. 10a, b, 11a) rather than with OIB. The TGU eclogites are associated with continental material, including Bt-gneiss and granitic gneiss and the eclogites have a reported within plate basalt character (Bucher et al., 2019, 2020; Weber & Bucher, 2015).

The REE patterns of all meta-gabbros (Fig. 12b) are similar and all show a prominent positive Eu anomaly. The meta-gabbros contain less REE compared with the meta-basalts. The DBN meta-gabbros have generally higher REE concentrations than ZSU meta-gabbros but display the same general pattern (Fig. 12b), which is, however, not necessarily evidence for a genetic connection. DBN meta-gabbro data from the south wall of the Matterhorn (Cervino samples of Manzotti et al., 2017) are similar to the data from the west wall presented here. Published data from meta-gabbros of the Tsaté nappe (Manzoti et al., 2017) are consistent with a mid-ocean ridge origin for the gabbros.

The effects of post-magmatic alteration on the REE patterns can be complex and difficult to be recognized. Hydrothermal seawater derived fluids can be enriched in heavy REE leaving behind light REE enriched alteration products. Critical for the REE alteration is the mineral assemblage of the altered basalts. If it contains zeolites, e.g. produced by reaction 2 discussed above, the interaction fluids acquire heavy REE (Aggarwal et al., 1994) and the residual altered and hydrated mafic igneous rocks modify their original REE pattern (Hopper & Smith, 1996). The REE of the SMN (Minugrat) eclogites have been immobile in the core region of the lenses and bands and REE metasomatism is restricted to the outermost shells of the eclogite occurrences (Eisele et al., 1997). Low-T alteration with surface derived fluids tends to leach heavy REE (Eu-Lu) proportionally (stoichiometrically) to the concentration of the REE in the rock thus it cannot be proven in the residual rock (Möller et al., 1997). The experimental data show that the fluids do not, however, dissolve light REE (La-Sm) leaving a residue with lowered heavy REE and passively enriched light REE. Low-T alteration has affected the Matterhorn meta-gabbro during low-grade Alpine metamorphism (< 300 °C) (Fig. 6). The described REE feature is not present in the REE data for the DBN meta-gabbro. In contrast, the light REE are flat and the heavy REE steeper than reference rocks (Fig. 12) suggesting that the pattern is of igneous origin and the observed low-grade alteration did not modify the igneous REE pattern. Subduction zone fluids that modified the bulk and trace element features of the ZSU eclogites did not disturb their REE patterns (Fig. 12). This is in agreement with the REE patterns of Jurassic Tethian sediments of the ZSU, which have not been modified by high- to ultra-high pressure Alpine metamorphism (Mahlen et al., 2005). The data suggest that the REE concentrations remain characterized by the primary rock forming process either igneous or sedimentary.

The ZSU eclogites and particularly the Allalin meta-gabbro show evidence for massive fluid-rock interaction during subduction and exhumation (Bucher & Grapes, 2009). The ZSU eclogites and meta-gabbros are all uniformly very low in K although they demonstrably experienced massive Na and Mg enrichment coupled with

Ca loss, suggesting that the Na-metasomatism was not linked to K-Rb depletion. In contrast to the ZSU HP rocks, TGU and SMN eclogites contain some K-mica phengite carrying the bulk potassium of the rocks (Fig. 13). This relatively high K likely represents a primary igneous feature in the case of the SMN eclogites, which show very little variation on the K vs. Ba/Rb diagram. The significant spread of TGU eclogites data in Fig. 13 is best explained by infiltration of K-Rb fluids derived from Grt-micaschist and Bt-gneiss associated with the TGU eclogites (Bucher et al., 2020).

6 Conclusions

The metamorphic gabbros and basalts occurring in continental and ophiolitic nappes of the Zermatt region of the Western Alps show distinct composition patterns typical of the geotectonic environment where the rocks originally formed.

The magmas of meta-volcanic eclogites of the Zermatt region formed in three different geotectonic environments. The TGU eclogites originally developed in a within plate setting (WPTB). They are hypersthene normative and show compositional features distinctly different from ZSU and SMN eclogites. The SMN eclogites show a clear MORB signature and the option that they represent the source of the tectonic TGU eclogite slivers can be rejected. The ZSU eclogites show distinct effects of interaction with both hydrothermal seafloor fluids and subduction zone fluids altering the primary basalt composition. The analyzed ZSU eclogites show normative nepheline, which is probably not a primary magmatic feature but the result of the post-magmatic alteration of the rocks. However, the preserved REE and trace element patterns suggest that the ZSU eclogites formed from enriched MORB-type seafloor basalts.

Supplementary Information

The online version contains supplementary material available at https://doi.org/10.1186/s00015-021-00390-w.

Additional file 1: Table S1. Major element composition of metamorphic basalts and gabbros. **Table S2.** Trace element composition of metamorphic basalts and gabbros. **Table S3.** REE composition of metamorphic basalts. **Table S4.** REE composition of metamorphic gabbros

Acknowledgements
We are grateful to Prof. Dr. Rudolf Hänny (University of Basel) for digging out samples from Peter Bearth and Meinert Rahn for this study, to Isolde Schmidt for XRF analyses and to Sarah Thyret from SGS for efficient handling of our samples.

Authors' contributions
KB carried out fieldwork, phase equilibrium computations, drafted the figures and the manuscript. IS carried out fieldwork, assembled the chemical data and tables, revised the manuscript. Both authors read and approved the final manuscript.

Funding
Open Access funding enabled and organized by Projekt DEAL.. Not applicable.

Availability of data and materials
Not applicable.

Declarations

Competing interests
The authors declare that they have no competing interests.

Received: 18 May 2020 Accepted: 18 March 2021
Published online: 12 April 2021

References

Aggarwal, J. K., Palmer, M. R., & Ragnarsdottir, K. V. (1994). Rare earth elements in Icelandic hydrothermal fluids Goldschmidt Conference Edinburgh. *Mineralogical Magazine, 58A*, 5–6.

Amato, J. M., Baumgartner, L., Johnson, C. M., & Beard, M. (1999). Rapid exhumation of the Zermatt-Saas ophiolite deduced from high-pressure Sm-Nd and Rb-Sr geochronology. *Earth and Planetary Science Letters, 171*, 425–438.

Angiboust, S., Agard, P., Jolivet, L., & Beyssac, O. (2009). The Zermatt-Saas ophiolite: The largest (60-km wide) and deepest (c. 70–80 km) continuous slice of oceanic lithosphere detached from a subduction zone? *Terra Nova, 21*, 171–180.

Ansermet, S. (2012). *Mines et minéraux du Valais. II. Anniviers et Tourtemagne. Musée de la Nature (Sion), Musée Cantonal de Géologie (Lausanne), With contributions of N. Meisser* (p. 374). Switzerland: Editions Porte-Plumes (Ayer), Valais.

Arevalo, R., Jr., & McDonough, W. F. (2010). Chemical variations and regional diversity observed in MORB. *Chemical Geology, 271*, 70–85.

Argand, E. (1908). Carte géologique du massif de la Dent Blanche, 1:50.000, carte spéciale 52. *Materiaux pour la carte géologique de la Suisse*.

Baletti, L., Zanoni, D., Spalla, M. I., & Gosso, G. (2012). Structural and petrographic map of the Sassa gabbro complex (Dent Blanche nappe, Austroalpine tectonic system, Western Alps, Italy). *Journal of Maps, 8*, 413–430.

Barnicoat, A. C., & Fry, N. (1986). High-pressure metamorphism of the Zermatt-Saas ophiolite zone, Switzerland. *Journal of the geological Society of London, 143*, 607–618.

Barnicoat, A. C., Rex, D. C., Guise, P. G., & Cliff, R. A. (1995). The timing of and nature of greenschist facies deformation and metamorphism in the upper Pennine Alps. *Tectonics, 14*, 279–293.

Bearth, P. (1953). Karte der Schweiz 535 (1:25000). *Geologischer Atlas der Schweiz, Blatt 29 Zermatt*.

Bearth, P. (1959). Über Eklogite, Glaukophanschiefer und metamorphe Pillowlaven. *Schweizerische Mineralogische und Petrographische Mitteilungen, 39*, 267–286.

Bearth, P. (1963). Chloritoid und Paragonit aus der Ophiolith-Zone von Zermatt-Saas Fee. *Schweizerische Mineralogische und Petrographische Mitteilungen, 43*, 269–286.

Bearth, P. (1967). Die Ophiolithe der Zone von Zermatt-Saas Fee. *Beiträge zur geologischen Karte der Schweiz N.F., 132*, 130.

Bearth, P. (1978). *Geologischer Atlas der Schweiz 1:25'000, Blatt N° 71: St. Niklaus (LK 1308)*. Bundesamt für Landestopografie.

Bearth, P., & Schwander, H. (1981). The post-Triassic sediments of the ophiolite zone Zermatt-Saas Fee and the associated manganese mineralizations. *Eclogae Geologicae Helvetiae, 74*, 189–205.

Bearth, P., & Stern, W. (1971). Zum Chemismus der Eklogite und Glaukophanite von Zermatt. *Schweizerische Mineralogische und Petrographische Mitteilungen, 51*, 349–359.

Bearth, P., & Stern, W. (1979). Zur Geochemie von Metapillows der Region Zermatt-Saas. *Schweizerische Mineralogische und Petrographische Mitteilungen, 59*, 349–373.

Bebout, G. E. (2007). Metamorphic chemical geodynamics of subduction zones. *Earth and Planetary Science Letters, 260*, 373–393.

Beltrando, M., Rubatto, D., & Manatschal, G. (2010). From passive margins to orogens: The link between ocean-continent transition zones and (ultra) high-pressure metamorphism. *Geology, 38*, 559–562.
Berman, R. B. (1988). Internally consistent thermodynamic data for minerals in system: Na2O-K2O-CaO-MgO-FeO-Fe2O3-Al2O3-SiO2-TiO2-H2O-CO2. *Journal of Petrology, 29*, 445–522.
Bowtell, S. A., Cliff, R. A., & Barnicoat, A. C. (1994). Sm-Nd isotopic evidence on the age of eclogitization in the Zermatt-Sass ophiolite. *Journal of Metamorphic Geology, 12*, 187–196.
Bucher, K., Dal Piaz, G. V., Oberhänsli, R., Gouffon, Y., Martinotti, G., & Polino, R. (2003). Blatt 1347 Matterhorn. *Geologischer Atlas der Schweiz 1:25000, Karte 107*.
Bucher, K., Dal Piaz, G. V., Oberhänsli, R., Gouffon, Y., Martinotti, G., & Polino, R. (2004). Blatt 1347 Matterhorn. *Geologischer Atlas der Schweiz 1:25000, Erläuterungen zur Karte 107, 73*.
Bucher, K., Fazis, Y., de Capitani, C., & Grapes, R. (2005). Blueschists, eclogites and decompression assemblages of the Zermatt-Saas ophiolite: High-pressure metamorphism of subducted Tethys lithosphere. *American Mineralogist, 90*, 821–835.
Bucher, K., & Grapes, R. (2009). The eclogite-facies allalin gabbro of the Zermatt-Saas Ophiolite, Western Alps: A record of subduction zone hydration. *Journal of Petrology, 50*, 1405–1442.
Bucher, K., & Stober, I. (2010). Fluids in the upper continental crust. *Geofluids, 10*, 241–253.
Bucher, K., & Weisenberger, T. (2013). Fluid induced mineral composition adjustments during exhumation: The case of Alpine stilbite. *Contributions to Mineralogy and Petrology, 166*, 1489–1503.
Bucher, K., Weisenberger, T., Weber, S., & Klemm, O. (2019). Decoding the complex internal chemical structure of garnet porphyroblasts from the Zermatt area, Western Alps. *Journal of metamorphic Geology, 37*, 1151–1169.
Bucher, K., Weisenberger, T., Weber, S., Klemm, O., & Corfu, F. (2020). The Theodul Glacier Unit, a slab of pre-Alpine rocks in the Alpine meta-ophiolite of Zermatt-Saas Western Alps. *Swiss Journal of Geosciences, 113*(1), 22p. https://doi.org/10.1186/s00015-020-00354-6.
Carmichael, I. S. E., Turner, F. J., & Verhoogen, J. (1974). *Igneous Petrology*. (p. 739). McGraw-Hill.
Charlot-Prat, F. (2005). An undeformed ophiolite in the Alps: Field and geochemical evidence for a link between volcanism and shallow plate tectonic processes. In: Fougler G. R., Natland, J. H., Presnall, D. C., & Anderson, D. L., (Eds), Plates Plumes and Paradigms. Geological Society of America Specials, 388, 751–780.
Coish, R., Kim, J., Twelker, E., Zolkos, S., & Walsh, G. (2015). Geochemistry and origin of metamorphosed mafic rocks from the Lower Paleozoic Moretown and Cram Hill Formations of north-central Vermont: Delamination magmatism in the western New England Appalachians. *American Journal of Science, 315*, 809–845.
Cruciani, G., Franceschelli, M., Langone, A., Puxeddu, M., & Scodina, M. (2015). Nature and age of pre-Variscan eclogite protoliths from the Low- to Medium-Grade Metamorphic Complex of north–central Sardinia (Italy) and comparisons with coeval Sardinian eclogites in the northern Gondwana context. *Journal of the Geological Society, 172*, 792–807.
Dal Piaz, G. V., Bistacchi, A., Gianotti, F., Monopoli, B., & Passeri, L. (2015). Note illustrative della carta Geologica d'Italia alla scala 1:50000. Foglio 070. *Cervino. Servizio Geologico d'Italia, 070*, 1–431.
Dal Piaz, G. V., Cortiana, G., Del Moro, A., Martin, S., Pennacchioni, G., & Tartarotti, P. (2001). Tertiary age and paleostructural inferences of the eclogitic imprint in the Austroalpine outliers and Zermatt-Saas ophiolite, western Alps. *International Journal of Earth Sciences, 90*, 668–684.
Dal Piaz, G. V., De Vecchi, G., & Hunziker, J. (1977). The Austroalpine layered gabbros of the Matterhorn and Mont Collon - Dents de Bertol. *Schweizerische Mineralogische und Petrographische Mitteilungen, 57*, 59–81.
de Capitani, C., & Petrakakis, K. (2010). The computation of equilibrium assemblage diagrams with Theriak/Domino software. *American Mineralogist, 95*, 1006–1016.
de Meyer, C., Baumgartner, L. P., Beard, B. L., & Johnson, C. M. (2014). Rb-Sr ages from phengite inclusions in garnets from high pressure rocks of the Swiss Western Alps. *Earth and Planetary Science Letters, 395*, 205–216.
Desmurs, L., Müntener, O., & Manatschal, G. (2002). Onset of magmatic accretion within a magma-poor rifted margin: A case study from the Platta ocean-continent transition, eastern Switzerland. *Contributions to Mineralogy and Petrology, 144*, 365–382.
Eisele, J., Geiger, S., & Rahn, M. (1997). Chemical characterization of metabasites from the Turtmann valley (Valais, Switzerland): Implications for their protoliths and geotectonic origin. *Schweizerische Mineralogische und Petrographische Mitteilungen, 77*, 403–417.
Ellenberger, F. (1953). La série du Barrhorn et les rétrocharriages penniques: *Comptes rendus de l'Académie des Sciences de Paris, 236, 218-220*.
Ernst, W. G., & Dal Piaz, G. V. (1978). Mineral parageneses of eclogitic rocks and related mafic schists of the Piemonte Ophiolite nappe, Breuil-Saint-Jacques area, Italian Western Alps. *American Mineralogist, 63*, 621–640.
Escher, A., Masson, H., & Steck, A. (1993). Nappe geometry in the Western Swiss Alps. *Journal of Structural Geology, 15*, 501–509.
Floyd, P. A., & Winchester, J. A. (1978). Identification and discrimination of altered and metamorphosed volcanic rocks using immobile elements. *Chemical Geology, 21*, 291–306.
Fourny, A., Weis, D., & Scoates, J. S. (2019). Isotopic and Trace Element Geochemistry of the Kiglapait Intrusion, Labrador: Deciphering the Mantle Source, Crustal Contributions and Processes Preserved in Mafic Layered Intrusions. *Journal of Petrology, 60*, 553–590.
Franciosi, L., D'Antonio, M., Fedele, L., Guarino, V., Tassinari, C. C. G., de Gennaro, R., & Cucciniello, C. (2019). Petrogenesis of the Solanas gabbro-granodiorite intrusion, Sàrrabus (southeastern Sardinia, Italy): Implications for Late Variscan magmatism. *International Journal of Earth Sciences, 108*, 989–1012.
Furnes, H., Dilek, Y., Zhao, G., Safonova, I., & Santosh, M. (2020). Geochemical characterization of ophiolites in the Alpine-Himalayan Orogenic Belt: Magmatically and tectonically diverse evolution of the Mesozoic Neotethyan oceanic crust. *Earth-Science Reviews, 208*, 103258.
Gale, A., Dalton, C. A., Langmuir, C. H., Yongjun, Su., & Schilling, J.-G. (2013). The mean composition of ocean ridge basalts. *Geochemistry, Geophysics, Geosystems, 14*, 489–518.
Gale, G. H., & Roberts, D. (1974). Trace element geochemistry of Norwegian Lower Paleozoic basic volcanics and its tectonic implications. *Earth and Planetary Science Letters, 22*, 380–390.
Ganguin, J. (1988). *Contribution à la caractérisation du métamorphisme polyphases de la zone de Zermatt-Saas Fee (Alps Valaisannes)*. (p. 312). PhD, ETH, Zürich, Switzerland.
Grenne, T., & Roberts, D. (1980). Geochemistry and volcanic setting of the Ordovician Forbordfjell and Jonsvatn greenstones, Trondheim region, central Norwegian Caledonides. *Contributions to Mineralogy and Petrology, 74*, 375–386.
Groppo, C., Beltrando, M., & Compagnoni, R. (2009). The P-T path of the ultra-high pressure Lago di Cignana and adjoining high-pressure meta-ophiolitic units: Insights into the evolution of the subducting Tethyan slab. *Journal of Metamorphic Geology, 27*, 207–231.
Hernández-Uribe, D., Palin, R. M., Cone, K. A., & Cao, W. (2020). Petrological Implications of seafloor hydrothermal alteration of subducted mid-ocean ridge basalt. *Journal of Petrology*. https://doi.org/10.1093/petrology/egaa086.
Hollocher, K., Robinson, P., Seaman, K., & Walsh, W. (2016). Ordovician-Early Silurian intrusive rocks in the northwest part of the Upper Allochthon, Mid-Norway: Plutons of an Iapetan Volcanic Arc Complex. *American Journal of Science, 316*, 925–980.
Hollocher, K., Robinson, P., Walsh, E., & Roberts, D. (2012). Geochemistry of amphibolite-facies volcanics and gabbros of the Støren Nappe in extensions west and southwest of Trondheim, Western Gneiss Region, Norway: A key to correlations and paleotectonic settings. *American Journal of Science, 312*, 357–416.
Hopper, D. J., & Smith, I. E. M. (1996). Petrology of the gabbro and sheeted basaltic intrusives at North Cape, New Zealand. *New Zealand Journal of Geology and Geophysics, 39*, 389–409.
Irvine, T. N., & Baragar, W. R. A. (1971). A Guide to the Chemical Classification of the Common Volcanic Rocks. *Canadian Journal of Earth Science, 8*, 523–548.
Keller, J. M., de Capitani, C., & Abart, R. (2005). A quaternary solution model for white micas based on natural coexisting phengite–paragonite pairs. *Journal of Petrology, 46*, 2129–2144.
Kramer, J., Abart, R., Müntener, O., Schmid, St., & M. & Stern, W-B. . (2003). Geochemistry of metabasalts from ophiolitic and adjacent distal continental margin units: Evidence from yje Monte Rosa region (Swiss

and Italian Alps). *Schweizerische Mineralogische und Petrographische Mitteilungen, 83*, X1–X24.
Kuno, H. (1969). Mafic and ultramafic nodules in basaltic rocks of Hawaii. *Geological Society of America Memoirs, 115*, 189–234.
Lagabrielle, Y., & Cannat, M. (1990). Alpine Jurassic ophiolites resemble the modern central Atlantic basement. *Geology, 18*(4), 319–322.
Lagabrielle, Y., & Lemoine, M. (1997). Alpine, Corsican and Apennine ophiolites: The slow-spreading ridge model. Ophiolites des Alpes, de Corse et de l'Apennin : le modèle des dorsales lentes. Comptes Rendus de l'Académie des Sciences Series IIA Earth and Planetary Science, 325(12): 909–920.
Lapen, T. J., Johnson, C. M., Baumgartner, L. P., Mahlen, N. J., Beard, B. L., & Amato, J. M. (2003). Burial rates during prograde metamorphism of an ultra-high-pressure terrane: An example from Lago di Cignana, western Alps, Italy. *Earth and Planetary Science Letters, 215*, 57–72.
Le Bas, M. J., Le Maitre, R. W., Streckeisen, A., & Zanettin, B. (1986). A chemical classification of volcanic rocks based on the total alkali–silica diagram. *Journal of Petrology, 27*, 745–750.
Le Maitre, R., Streckeisen, A., Zanettin, B., Le Bas, M., Bonin, B., & Bateman, P. (Eds.). (2002). *Igneous Rocks: A Classification and Glossary of Terms: Recommendations of the International Union of Geological Sciences Subcommission on the Systematics of Igneous Rocks* (2nd ed.). Cambridge University Press.
Li, X.-H., Faure, M., Rossi, P., Lin, W., & Lahondère, D. (2015). Age of Alpine Corsica ophiolites revisited: Insights from in situ zircon U-Pb age and O-Hf isotopes. *Lithos, 220–223*, 179–190.
Li, X.-P., Rahn, M., & Bucher, K. (2004a). Serpentinites of the Zermatt-Saas ophoilite complex and their texture evolution. *Journal of Metamorphic Geology, 22*, 159–178.
Li, X.-P., Rahn, M., & Bucher, K. (2004b). Metamorphic processes in rodingites of the Zermatt-Saas Ophiolites. *International Geology Review, 46*, 28–51.
Li, X.-P., Rahn, M., & Bucher, K. (2008). Eclogite-facies metarodingites: Phase relations in the system SiO_2-Al_2O_3-FeO-Fe_2O_3-MgO-CaO-CO_2-H_2O; an example from the Zermatt-Saas Ophiolite. *Journal of Metamorphic Geology, 26*, 347–364.
Loeschke, J. (1976). Major element variations in Ordovician pillow lavas of the Støren Group, Trondheim region, Norway . *Norsk Geologisk Tidsskrift, 56*(Special Supplement 2), 141–159.
Lyubetskaya, T., & Korenaga, J. (2007). Chemical composition of Earth's primitive mantle and its variance: 1 Method and results . *Journal of Geophysical Research, 112*, B03211. https://doi.org/10.1029/2005JB004223.
Mahlen, N. J., Johnson, C. M., Baumgartner, L. P., & Beard, B. L. (2005). Provenance of Jurassic Tethyan sediments in the HP/UHP Zermatt-Saas ophiolite, western Alps. *GSA Bulletin, 117*, 530–544.
Manatschal, G., Sauter, D., Karpoff, A. M., Masini, E., Mpohn, G., & Lagabrielle, Y. (2011). The Chenaillet Ophiolite in the French/Italian Alps: An acient analogue for an Oceanic Core Complex? *Lithos, 124*(3–4), 169–184.
Manzotti, P., Ballèvre, M., & Dal Piaz, G. V. (2017). Continental gabbros in the Dent Blanche Tectonic System (Western Alps): From the pre-Alpine crustal structure of the Adriatic palaeo-margin to the geometry of an alleged subduction interface. *Journal of the Geological Society, 174*, 541–556.
Manzotti, P., Ballèvre, M. Z., Robyr, M., & Engi, M. (2014). The tectonometamorphic evolution of the Sesia-Dent Blanche nappes (internal Western Alps): Review and synthesis. *Swiss Journal of Geosciences, 107*, 309–336.
Manzotti, P., Rubatto, D., Zucali, M., El Korh, A., Cenki-Tok, B., Ballevre, M., & Engi, M. (2018). Permian magmatism and metamorphism in the Dent Blanche nappe: Constraints from field observations and geochronology. *Swiss Journal of Geosciences, 111*, 79–97.
Marotta, A. M., Roda, M., Conte, K., & Spalla, M. I. (2018). Thermo-mechanical numerical model of the transition from continental rifting to oceanic spreading: The case study of the Alpine Tethys. *Geological Magazine, 155*, 250–279.
Marthaler, M., Sartori, M., & Escher, A. (2008). Karte der Schweiz 1307 (1:25000). *Geologischer Atlas der Schweiz, Blatt 122 Vissoie*.
McDonough, W. F., & Sun, S.-S. (1995). The composition of the Earth. *Chemical Geology, 120*, 223–253.
Meschede, M. (1986). A method of discriminating between different types of mid-ocean ridge basalts and continental tholeiites with the Nb-Zr-Y diagram. *Chemical Geology, 56*, 207–218.
Meyre, C., De Capitani, C., & Partsch, J. H. (1997). A ternary solid solution model for omphacite and its application to geothermobarometry of eclogites from the Middle Adula nappe (Central Alps, Switzerland). *Journal of Metamorphic Geology, 15*, 687–700.
Möller, P., Stober, I., & Dulski, P. (1997). Seltenerdelement-, Yttrium-Gehalte und Bleiisotope in Thermal- und Mineralwässern des Schwarzwaldes (REE, Y concentration and Pb isotopes in thermal and mineral waters of the Black Forest region, Germany). *Gundwasser, 3*, 118–132.
Monjoie, P., Bussy, F., Lapierre, H., & Pfeifer, H.-R. (2005). Modeling of in-situ crystallization processes in the Permian mafic layered intrusion of Mont Collon (Dent Blanche nappe, western Alps). *Lithos, 83*, 317–346.
Monjoie, P., Bussy, F., Lapierre, H., Schaltegger, U., Pfeifer, H.-R., & Mulch, A. (2007). Contrasting magma types and timing of intrusion in the Permian layered mafic complex of Mont Collon (Western Alps, Valais, Switzerland): Evidence from U/Pb zircon and $^{40}Ar/^{39}Ar$ amphibole dating. *Swiss Journal of Geosciences, 100*, 125–135.
Mullen, E. D. (1983). $MnO/TiO_2/P_2O_5$: A minor element discriminant for basaltic rocks of oceanic environments and its implications for petrogenesis. *Earth and Planetary Science Letters, 62*, 53–62.
Neo, N., Yamazaki, S., & Miyashita, S. (2009). Data report: Bulk rock compositions of samples from the IODP Expedition 309/312 sample pool, ODP Hole 1256D. In Teagle, D.A.H., Alt, J.C., Umino, S., Miyashita, S., Banerjee, N.R., Wilson, D.S., and the Expedition 309/312 Scientists, Proc. IODP, 309/312. Integrated Ocean Drilling Program Management International, Inc. https://doi.org/10.2204/iodp.proc.309312.204.2009.
Oberhänsli, R. (1982). The P-T history of some pillow lavas from Zermatt. *Ofioliti, 2*, 431–436.
Pearce, J. A., & Cann, J. R. (1973). Tectonic setting of basic volcanic rocks determined using trace element analyes. *Earth and Planetary Science Letters, 19*, 290–300.
Pedersen, R. B., & Hertogen, J. (1990). Magmatic evolution of the Karmøy Ophiolite Complex, SW Norway: Relationships between MORB–IAT–boninitic– calc-alkaline and alkaline magmatism. *Contributions to Mineralogy and Petrology, 104*, 277–293.
Pfeifer, H. R., Colombi, A., & Ganguin, J. (1989). Zermatt-Saas and Antrona Zone: A petrographic and geochemical comparison of polyphase metamorphic ophiolites of the West-Central Alps. *Schweizerische Mineralogische und Petrographische Mitteilungen, 69*, 217–236.
Plank, T., & Langmuir, C. H. (1988). An evaluation of the global variations in the major element chemistry of arc basalts. *Earth and Planetary Science Letters, 90*, 349–370.
Pleuger, J., Roller, S., Walter, J. M., Jansen, E., & Froitzheim, N. (2007). Structural evolution of the contact between two Penninic nappes (Zermatt-Saas zone and Combin zone, Western Alps) and implications for the exhumation mechanism and palaeogeography. *International Journal of Earth Sciences, 96*, 229–252.
Putnis, A., & Austrheim, H. (2020). Fluid-induced processes: Metasomatism and metamorphism. *Geofluids, 10*, 254–269.
Rahn, M. (1991). Eclogites from Minugrat, Siviez-Mischabel nappe (Valais, Switzerland). *Schweizerische Mineralogische und Petrographische Mitteilungen, 71*, 415–426.
Rebay, G., Spalla, M. I., & Zanoni, D. (2012). Interaction of deformation and metamorphism during subduction and exhumation of hydrated oceanic mantle: Isights from the Western Alps. *Jounal of Metamorphic Geology, 30*, 687–702.
Roda, M., Regorda, A., Spalla, M. I., & Marotta, A. M. (2018). What drives Alpine Tethys opening? Clues from the review of geological data and model predictions. *Geological Journal, 2018*, 1–19.
Rubatto, D., Gebauer, D., & Fanning, M. (1998). Jurassic formation and Eocene subduction of the Zermatt-Saas-Fee ophiolites: Implications for the geodynamic evolution of the Central and Western Alps. *Contributions to Mineralogy and Petrology, 132*, 269–287.
Rubatto, D., & Hermann, J. (2003). Zircon formation during fluid circulation in eclogites (Monviso, Western Alps): Implications for Zr and Hf budget in subduction zones. *Geochimica et Cosmochimica Acta, 67*, 2173–2187.
Schmidt, M. E., Schrader, Ch. M., Crumpler, L. S., Rowe, M. C., Wolff, J. A., & Boroughs, S. P. (2016). Megacrystic pyroxene basalts sample deep crustal gabbroic cumulates beneath the Mount Taylor volcanic field, New Mexico. *Journal of Volcanology and Geothermal Research, 316*, 1–11.

Seyfried, W. E., Mottl, M. J., & Bischoff, J. L. (1978). Seawater/basalt ratio effects on the chemistry and mineralogy of spilites from the ocean floor. *Nature, 275*, 211–213.
Shamberger, P. J., & Hammer, J. E. (2006). Leucocratic and Gabbroic Xenoliths from Hualalai Volcano Hawaii. *Journal of Petrology, 47*, 1785–1808.
Stampfli, G. M. (2000). Tethyan oceans. *Geological Society, London, Special Publications, 173*, 1–23.
Stampfli, G. M., & Marchant, R. H. (1997). Geodynamic evolution of the Tethyan margins of the Western Alps. In O. A. Pfifner, P. Lehner, P. Z. Heitzman, S. Mueller, & A. Steck (Eds.), *Deep Structure of the Swiss Alps - Results from NRP 20* (pp. 223-239). Birkhäuser AG.
Steck, A., Bigioggero, B., Dal Piaz, G. V., Escher, A., Martinotti, G., & Masson, H. (1999). *Carte tectonique des Alpes de Suisse occidentale et des régions avoisinantes, 1:100000, Geologische Spezialkarte, 123*. . Bundesamt für Wasser und Geologie.
Stober, I., & Bucher, K. (2005b). The upper continental crust, an aquifer and its fluid: Hydaulic and chemical data from 4 km depth in fractured crystalline basement rocks at the KTB test site. *Geofluids, 5*, 8–19.
Stober, I., & Bucher, K. (2005a). Deep-fluids: neptune meets pluto. *Hydrogeology Journal, 13*, 112–115.
Sun, S.-S., & McDonough, W. F. (1989). Chemical and isotopic systematics of oceanic basalts: Implications for mantle composition and processing. *Geological Society, London, Special Publications, 42*, 313–345.
Teagle, D. A. H., Alt, J. C., Umino, S., Miyashita, S., Banerjee, N. R., Wilson, D. S., & Expedition 309/312 Scientists (2009). Site 1256, Preliminary Results. *Proceedings of the Integrated Ocean Drilling Program, 309/312*.
Tsay, A., Zajacz, Z., Ulmer, P., & Sanchez-Valle, C. (2017). Mobility of major and trace elements in the eclogite-fluid system and element fluxes upon slab dehydration. *Geochimica et Cosmochimica Acta, 198*, 70–91.
van der Straaten, F., Halama, R., John, T., Schenk, V., Hauff, F., & Andersen, N. (2012). Tracing the effects of high-pressure metasomatic fluids and seawater alteration in blueschist-facies overprinted eclogites: Implications for subduction channel processes. *Chemical Geology, 292–293*, 69–87.
Villiger, S., Ulmer, P., Müntener, O., & Thompson, A. B. (2004). The liquid line of descent of anhydrous, mantle-derived, tholeiitic liquids by fractional and equilibrium crystallization—an experimental study at 1.0 GPa. *Journal of Petrology, 45*, 2369–2388.
Weber, S., & Bucher, K. (2015). An eclogite-bearing continental tectonic slice in the Zermatt-Saas high-pressure ophiolites at Trockener Steg (Zermatt, Swiss Western Alps). *Lithos, 232*, 336–359.
Weber, S., Sandmann, S., Miladinova, I., Fonseca, R. O. C., Froitzheim, N., Münker, C., & Bucher, K. (2015). Dating the initiation of Piemonte-Liguria ocean subduction: Lu–Hf garnet chronometry of eclogites from the theodul glacier unit (Zermatt–Saas Zone, Switzerland). *Swiss Journal of Geosciences, 108*, 183–199.
Weisenberger, T. B., Ingimarsson, H., Hersir, G. P., & Flóvenz, Ó. (2020). Cation-exchange capacity distribution within hydrothermal systems and its relation to the alteration mineralogy and electrical resistivity. *Energies, 13*, 5730.
Weisenberger, T., & Selbekk, R. S. (2009). Multi-stage zeolite facies mineralization in the Hvalfjördur area, Iceland. *International Journal of Earth Sciences, 98*, 985–999.
Whitney, D. L., & Evans, B. W. (2010). Abbreviations for names of rock-forming minerals. *American Mineralogist, 95*, 185–187.
Widmer, T., Ganguin, J., & Thompson, A. B. (2000). Ocean floor hydrothermal veins in eclogite facies rocks of the Zermatt-Saas Zone, Switzerland. *Schweizerische Mineralogische Petrographische Mitteilungen, 80*, 63–73.
Widmer, T., & Thompson, A. B. (2001). Local origin of high pressure vein material in eclogite facies rocks of the Zermatt-Saas Zone, Switzerland. *American Journal of Science, 301*, 627–656.
Will, T. M., Lee, S.-H., Schmädicke, E., Frimmel, H. E., & Okrusch, M. (2015). Variscan terrane boundaries in the Odenwald-Spessart Mid-German Crystalline Zone: New evidence from ocean ridge, intraplate and arc-derived metabasaltic rocks. *Lithos, 220–223*, 23–42.
Winchester, J. A., & Floyd, P. A. (1976). Geochemical magma type discrimination: application to altered and metamorphosed basic igneous rocks. *Earth and Planetary Science Letters, 28*, 459–469.
Yaliniz, M. K. (2008). A geochemical attempt to distinguish forearc and back arc ophiolites from the "supra-subduction" central Anatolian ophiolites (Turkey) by comparison with modern oceanic analogues. *Ofioliti, 33*, 119–129.

Publisher's Note